HEAVY QUARK PHYSICS AT LEP

P. S. Wells
* CERN
Geneva, Switzerland

ABSTRACT

The four LEP experiments each recorded about two million hadronic Z decays in the years 1990-1993. These provide access to a wide variety of topics in heavy quark physics, ranging from precise measurements in the electroweak sector to analyses involving specific decay modes with relatively small branching ratios. Results on the Z partial widths to heavy quarks, forward-backward asymmetries, $B^0\overline{B^0}$ mixing, and the lifetimes of different b hadrons are presented here. In addition, some examples are given of measurements which are both interesting in their own right and which can lead to a reduction in the systematic uncertainties in other heavy flavor analyses.

---

*

1 Introduction

Each of the LEP experiments has observed about two million hadronic Z decays between 1990 and 1993. Roughly two-fifths of these decays are via a $c\overline{c}$ or $b\overline{b}$ pair. The aim of this review is to give an impression of the scope of the analyses possible with these large samples of heavy quark events.

Decays of the Z to heavy quarks can be identified in several ways. The presence of electrons or muons in the final state with high momentum, p, due to the large boost of the b or c hadrons, and for $b\overline{b}$ events in particular with high transverse momentum with respect to the accompanying jet, p_T, are a well-known tag for heavy flavor events. The (partial) reconstruction of a heavy hadron is also used in many analyses, as will be seen throughout this review, and some use has been made at LEP of the characteristic differences in event shapes between heavy and light quark events. However, the most powerful tool for tagging heavy quark events relies on the long lifetimes of b and c hadrons. Combined with the typical boosts, this leads to decay lengths of a few millimeters. ALEPH, DELPHI, and OPAL have had silicon microvertex detectors since 1991, which can resolve these distances. Tagging algorithms are based either on the significant impact parameter (distance of closest approach of the track to the primary vertex) of several tracks in the event, or on a reconstructed secondary vertex significantly displaced from the primary vertex. An example is given in Fig. 1, and the relevant properties for b hadrons, compared with D^0 and D^+ mesons, are given in Table 1.

	B	D^+	D^0
Lifetime (ps)	1.6	1.0	0.4
$\langle x_E \rangle$	0.7	0.5	0.5
Charged multiplicity	5.5	2.2	2.2

Table 1: Properties of b hadrons and of D^0 and D^+ mesons. $\langle x_E \rangle$ is the mean hadron energy divided by the beam energy.

In Sec. 2, measurements of the properties of Z decay to heavy quarks are discussed. The following sections describe the mean lifetimes of different b hadrons and investigations of $B^0\overline{B^0}$ mixing. Finally, a few examples of analyses which are relevant to reducing the systematic uncertainties in the previous results are given.

2 Electroweak Measurements

2.1 Partial Widths and Asymmetries

In the Standard Model, radiative corrections to the process $e^+e^- \to Z \to f\overline{f}$ due to the propagator depend on the top quark mass squared, $M^2_{\rm top}$, and logarithmically on the Higgs boson mass, $\log(M_{\rm Higgs})$. However, there are unique vertex corrections for the process $Z \to b\overline{b}$, which also depend on $M^2_{\rm top}$, but are almost independent of $M_{\rm Higgs}$. In the ratio of partial widths, $R_b \equiv \Gamma_{b\overline{b}}/\Gamma_{\rm had}$, the propagator terms cancel, so that this gives a measure of $M_{\rm top}$ from the vertex corrections, independent of $M_{\rm Higgs}$. The variations in R_b for $50 \lesssim M_{\rm top} \lesssim 250$ GeV are of the order of 1%. In contrast, the other ratios, including $R_c \equiv \Gamma_{c\overline{c}}/\Gamma_{\rm had}$, are expected to be almost independent of $M_{\rm top}$. The partial widths are measured by counting the fraction of hadronic Z decays with a heavy quark tag and correcting for the efficiency and purity of the tagging method. This introduces systematic uncertainties, for example, due to branching ratios and the detection efficiencies. These uncertainties are much reduced using double-tagging methods (see Sec. 2.2).

The forward-backward asymmetry is defined by $A^f_{\rm FB} = (\sigma_F - \sigma_B)/(\sigma_F + \sigma_B)$, where σ_F and σ_B are the cross sections for the outgoing fermion, f, to go forwards or backwards relative to the direction of the incoming electron. To a good approximation, the differential cross section has the form:[1]

$$\frac{d\sigma}{d\cos\theta} \propto 1 + \cos^2\theta + \frac{8}{3}A^f_{\rm FB}\cos\theta, \tag{1}$$

where θ is the angle between the electron and fermion directions, and in practice, this expression defines the asymmetry for heavy flavor measurements. When the center-of-mass energy, $\sqrt{s}$, is equal to M_Z, then $A^f_{\rm FB}$ is related to the fermion vector and axial-vector couplings, v_f and a_f, by

$$A^f_{\rm FB} \approx A^{f,0}_{\rm FB} \equiv \frac{3}{4}\mathcal{A}_e\mathcal{A}_f \text{ where } \mathcal{A}_f = 2v_f a_f/(v_f^2 + a_f^2). \tag{2}$$

Small corrections[2] are applied to the observed asymmetry to derive the "pole" asymmetry, $A^{b,0}_{\rm FB}$. The asymmetry varies with center-of-mass energy around $\sqrt{s} = M_Z$ as a result of Z-photon interference.

The quark direction is estimated from the thrust axis. Some charge tag must be used to decide the direction of the quark and the antiquark, such as a final state lepton, a D meson, or a more inclusive "jet-charge" measure (see Sec. 2.5).

The effect of $B^0\overline{B^0}$ mixing is to reduce the observed $b\overline{b}$ asymmetry by a factor of $(1-2\chi)$, where χ is the time-integrated probability that a produced B^0 decays as a $\overline{B^0}$.*

2.2 Double-Tagging Methods

The most precise measurements of R_b use double-tagging methods based on counting the number of tagged hemispheres, N_t, and the number of events with two tagged hemispheres, N_{tt}, when the event is divided into two halves by a plane perpendicular to the thrust axis. These numbers are approximately given by:

$$N_t \approx 2N_{had}R_b\epsilon_b, \quad (3)$$

$$N_{tt} \approx N_{had}R_b{\epsilon_b}^2, \quad (4)$$

where ϵ_b is the b-quark tagging efficiency per hemisphere, and N_{had} is the total number of hadronic Z decays. This pair of equations can be solved for the two unknowns, R_b and ϵ_b, so that the b tagging efficiency is measured from the data. This avoids the need to evaluate the tagging efficiency of the algorithm used from Monte Carlo simulation and the associated systematic errors.

In reality, the situation is complicated by the presence of non-$b\overline{b}$ backgrounds, and from correlations in the tagging efficiency between hemispheres. Equations 3 and 4 become:

$$N_t = 2N_{had}(R_b\epsilon_b + R_c\epsilon_c + (1-R_b-R_c)\epsilon_{uds}), \quad (5)$$

$$N_{tt} = N_{had}(R_b{\epsilon_b}^2\rho_b + R_c{\epsilon_c}^2\rho_c + (1-R_b-R_c){\epsilon_{uds}}^2\rho_{uds}). \quad (6)$$

Here, ϵ_c and ϵ_{uds} are the tagging efficiencies per hemisphere for charm and light flavors, respectively. Equations 5 and 6 can still be solved for the efficiency ϵ_b and for the desired quantity R_b as before, but the correlations for each flavor, ρ_b, ρ_c, ρ_{uds}, and the tagging efficiencies, ϵ_c, ϵ_{uds}, must be estimated from Monte Carlo simulation. To reduce the associated systematic uncertainties, analyses are designed such that $\epsilon_b \gg \epsilon_c \gg \epsilon_{uds}$ and $\rho_b \approx 1$. Typical efficiency values are $\epsilon_b = 25\%$ and $\epsilon_c = 1\%$, with a b-purity of around 95% per hemisphere. The tagging algorithm is usually tuned to minimize the overall error from combining statistical and systematic uncertainties.

*The symbol B^0 is used in this note to refer to a B^0_d or B^0_s meson.

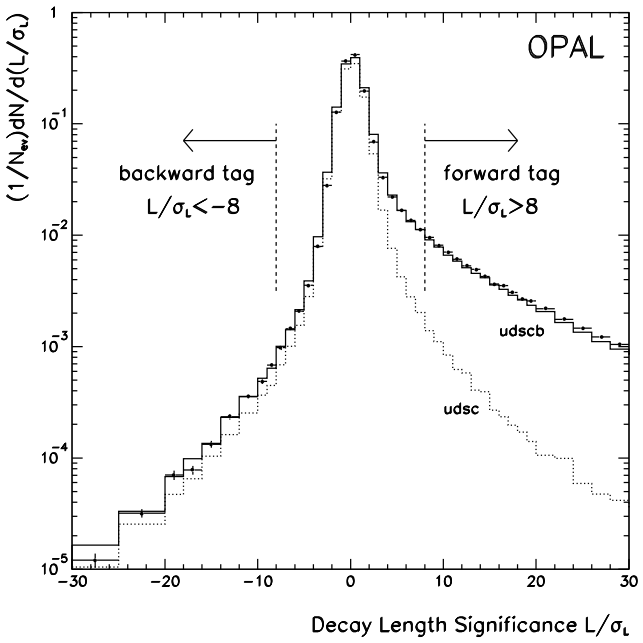

Figure 1: Decay length significance distributions from OPAL data (points) and Monte Carlo (solid). The light flavor contribution is indicated (dotted).

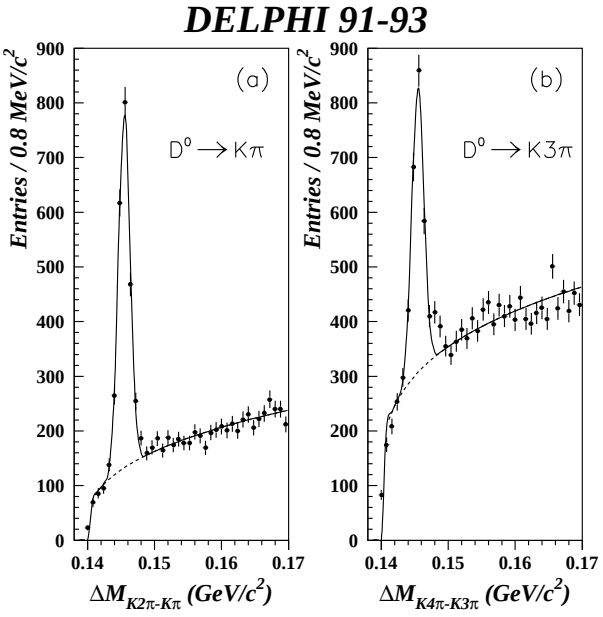

Figure 2: Mass difference distributions from DELPHI, for two D^0 decay modes, in events where the $D^\star$ candidate has $x_E > 0.25$.

The dominant systematic uncertainties arise from the knowledge of the charm background and the correlation between the hemispheres, and are listed here:

- Understanding of the modeling of the detector resolution directly affects the value of ϵ_c measured from a Monte Carlo simulation.
- The value of R_c must be either taken from experiment or assumed to have its Standard Model value, which is nearly independent of $M_{\rm top}$ and $M_{\rm Higgs}$.
- There are experimental uncertainties in the lifetimes of charm hadrons.
- Since the D^+ lifetime is about 2.5 times longer than the D^0 lifetime (see Table 1), the relative fractions of different charm hadrons produced in $Z \to c\overline{c}$ are a further source of uncertainty.
- The tagging efficiency for charm events is strongly affected by the charged multiplicity of charm hadron decays.
- The b-hadron momenta are correlated between hemispheres, and the presence of a hard gluon may result in the b and $\overline{\rm b}$ being in the same hemisphere.
- If the beam spot position or the error on its position are incorrect, this introduces correlations between the apparent lifetimes in each hemisphere.
- Efficiency variations intrinsic to a detector, such as back-to-back holes, also introduce a correlation.

In the context of systematic errors, it should be emphasized that $b\overline{b}$ and $c\overline{c}$ pairs produced from gluon splitting are not included in the definition of $\Gamma_{b\overline{b}}$ or $\Gamma_{c\overline{c}}$.

The lifetime tagging methods dominate.[3–5] The tagging efficiency can be improved by also allowing an identified high p, p_T lepton to tag a hemisphere. Tagging methods based on event shapes have also been used to measure R_b.[6,7]

2.3 Lepton-Fit Measurements

The first measurements of R_b at LEP used lepton p and p_T distributions to distinguish their different origins. These methods have continued to evolve.[8–11] The lepton fit analyses additionally provide information on the semileptonic branching ratio $\mathrm{Br}(b \to \ell)$ by analogy with the double-tagging method, assuming the lepton-identification efficiency is known. The analyses can be extended to measure R_c, the branching ratio $\mathrm{Br}(b \to c \to \ell)$, and $\langle x_E \rangle$ for b and c hadrons.

If the lepton charge is also considered, $A_{\rm FB}^{\rm b}$, $A_{\rm FB}^{\rm c}$, and time-integrated mixing can also be probed.[8,10–12] The dominant uncertainties in these analyses are from understanding the lepton identification, modeling of the semileptonic decay (especially the lepton momentum spectrum in the hadron rest frame), and those semileptonic branching ratios which are not directly measured. The parameters measured in the same fit are often highly correlated, which must be taken into account when combining them with other results.

2.4 Measurements Involving Charm Mesons

Reconstructed charm mesons have been used to measure $\rm R_c$[13,14] and $A_{\rm FB}^{\rm c}$.[15–17] The dominant systematic errors for $\rm R_c$ arise from uncertainties in the meson production and decay branching ratios, while the $A_{\rm FB}^{\rm c}$ measurements are statistics limited.

The decay $\rm D^{\star\pm} \to D^0\pi$ is readily identifiable due to the small mass difference of about 145 MeV between the $\rm D^\star$ and $\rm D^0$. The $\rm D^0$ is identified by its decays to $\rm K^-\pi^+$, $\rm K^-\pi^+\pi^0$, or $\rm K^-\pi^+\pi^-\pi^+$, and the $\rm D^0$ candidate combined with an additional pion. An example of the signal in the mass difference is shown in Fig. 2. To clean up the signal, one can use the track ionization, dE/dx, to distinguish pions from kaons or require that the $\rm D^0$ tracks come from the same vertex. The angle between the $\rm K^-$ and the $\rm D^0$ flight direction in the $\rm D^0$ rest frame also distinguishes signal and background, because the $\rm D^0$ decay is isotropic, while combinatorial background tends to be forward or backward peaked.

Just as leptons from $\rm b\overline{b}$ and $\rm c\overline{c}$ events are separated on a statistical basis according to their p and p_T, $\rm D^\star$ mesons can be separated according to their x_E. Lifetime, lepton, and event-shape information have also been used.

2.5 Jet-Charge Asymmetry Measurements

The b and c quarks can be selected by lifetime, lepton, or D-meson tags. Although a lifetime tag has no intrinsic charge properties, quark and antiquark can be distinguished by using a jet-charge measure,[18,19] $Q_{\rm jet}$, with definitions such as:

$$Q_{\rm jet} = \sum_i q_i \left(\frac{p_i^l}{E_{\rm beam}}\right)^\kappa \quad \text{or} \quad Q_{\rm jet} = \frac{\sum_i q_i (p_i^l)^\kappa}{\sum_i (p_i^l)^\kappa}. \tag{7}$$

The sum is over charged tracks, i, with charge q_i and longitudinal momentum components with respect to the jet p_i^l. The value of κ is tuned to give the best correspondence between $Q_{\rm jet}$ and the quark charge.

2.6 LEP Combined Results

A combined fit to LEP electroweak heavy quark results is motivated by the significant common systematic uncertainties for R_b, the problems of combining the lepton multiparameter fit results, and wanting to know the covariance matrix relating the average parameters.[2] To this end, a χ^2 of the form

$$\chi^2 = \sum_{ij} \delta_i V_{ij}^{-1} \delta_j \tag{8}$$

was minimized. Here, the δ_i are the differences between measurement i and the LEP average value for the parameter corresponding to measurement i, and V_{ij} is the covariance matrix relating all the measurements. This matrix takes into account the covariance matrices of the lepton fits and off-diagonal terms arising from common systematic errors. The LEP experiments provide the small corrections necessary to use an agreed set of common input parameters, and explicit dependences of the electroweak parameters on each other are included. This is particularly important for the dependence of R_b on R_c. After being combined, the asymmetries are corrected to give the pole asymmetries.

The input values from the experiments and the LEP average results are shown in Figs. 3, 4, 5, 7, and 8. The results for the partial widths are compared with the Standard Model prediction in Fig. 6, and the asymmetry measurements, including the measurements of the asymmetry off-peak, in Fig. 9. The measured value of R_b tends to favor a lower value of the top quark mass than other electroweak measurements, while there is, in general, good agreement with the Standard Model prediction for the asymmetries. The LEP combined results are:

$$\begin{aligned} R_b &= 0.2202 \pm 0.0020, \\ R_c &= 0.1583 \pm 0.0098, \\ {A_{FB}^b}^0 &= 0.0967 \pm 0.0038, \\ {A_{FB}^c}^0 &= 0.0760 \pm 0.0091. \end{aligned}$$

The correlations between the parameters are less than or of the order of 10%, apart from the correlation between R_b and R_c, which is about -40%. If R_c is fixed to its Standard Model value of 0.171, then the value of R_b becomes:

$$R_b(R_c = 0.171) = 0.2192 \pm 0.0018.$$

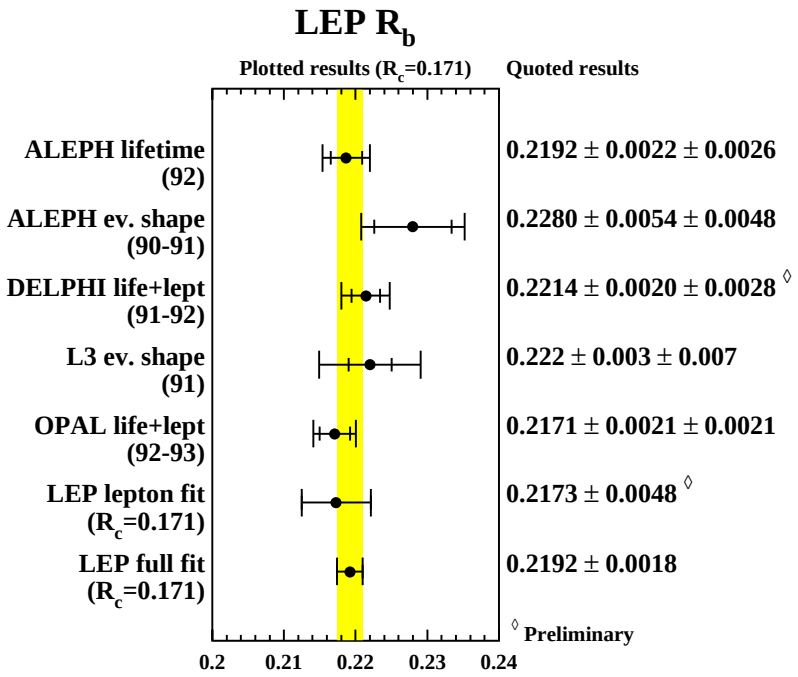

Figure 3: Measurements of R_b at LEP. Only the average value of R_b from multi-parameter lepton fits is shown here.

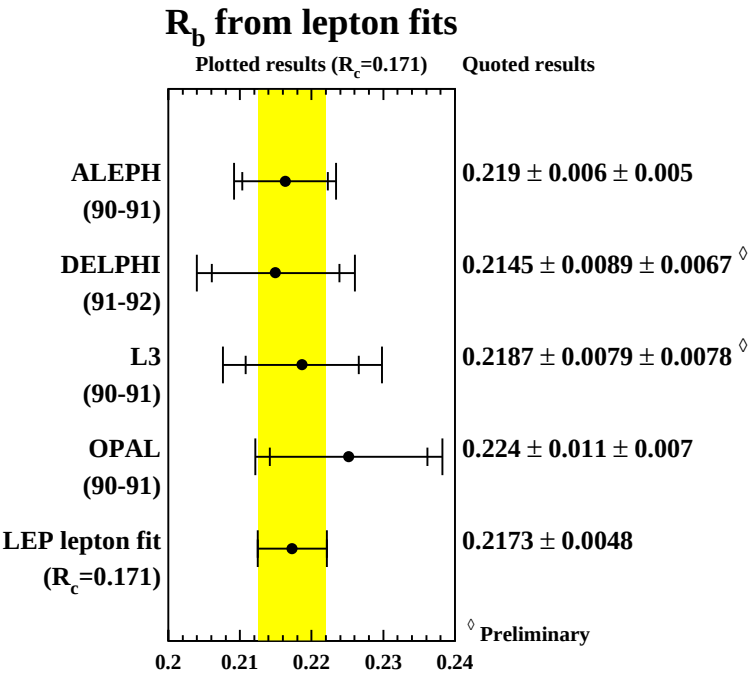

Figure 4: Measurements of R_b from multiparameter lepton fits at LEP.

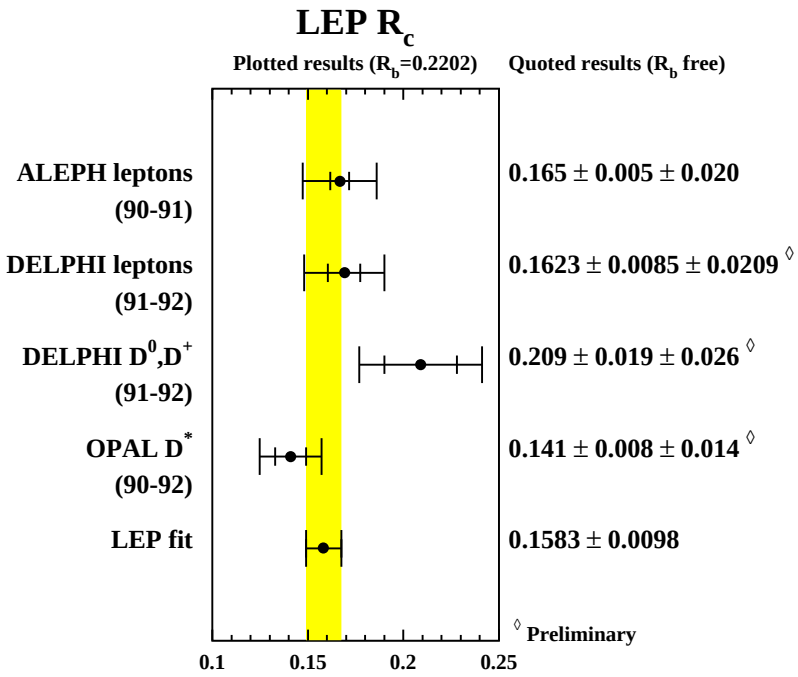

Figure 5: Measurements of R_c at LEP.

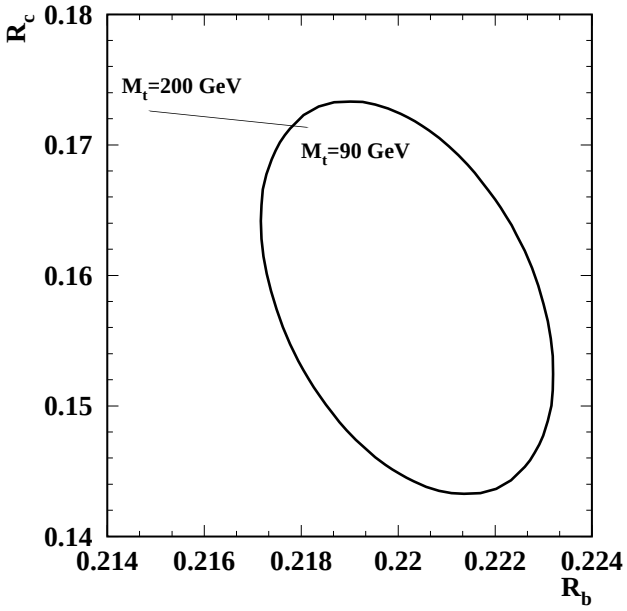

Figure 6: The 68% probability contour for the LEP average values of R_b and R_c. The Standard Model prediction for a range of top mass is also shown.

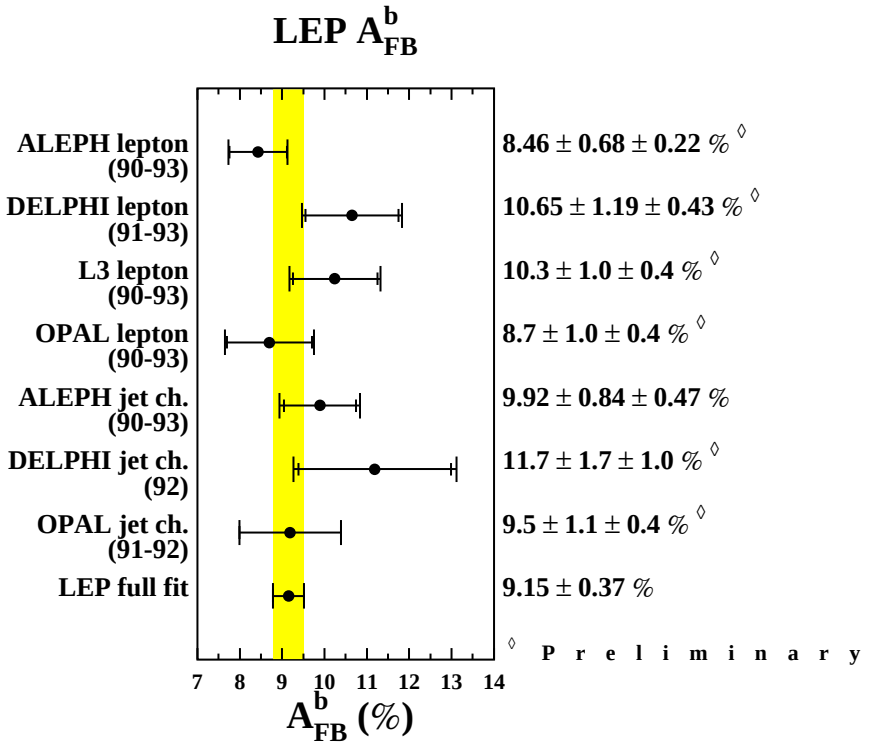

Figure 7: Measurements of $A_{\rm FB}^{\rm b}$ at LEP.

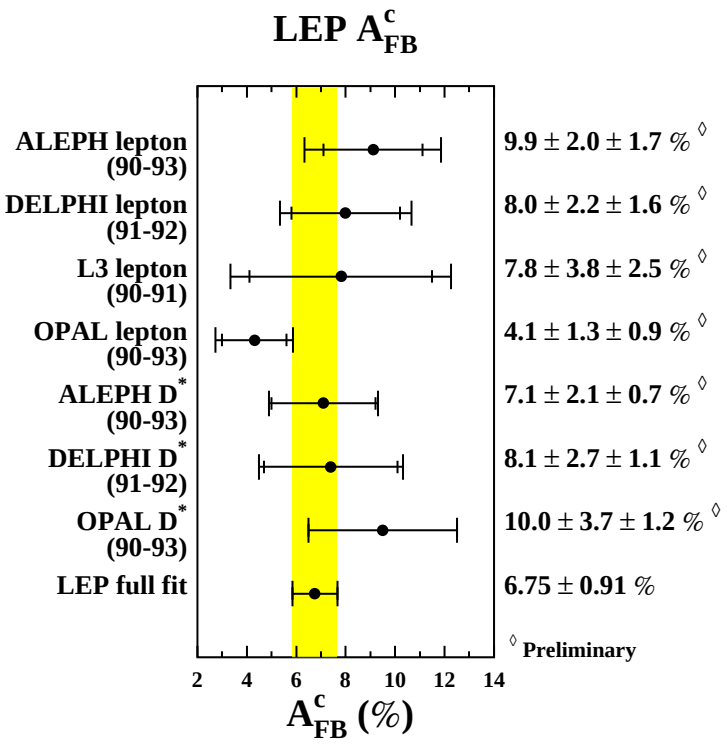

Figure 8: Measurements of $A_{\rm FB}^{\rm c}$ at LEP.

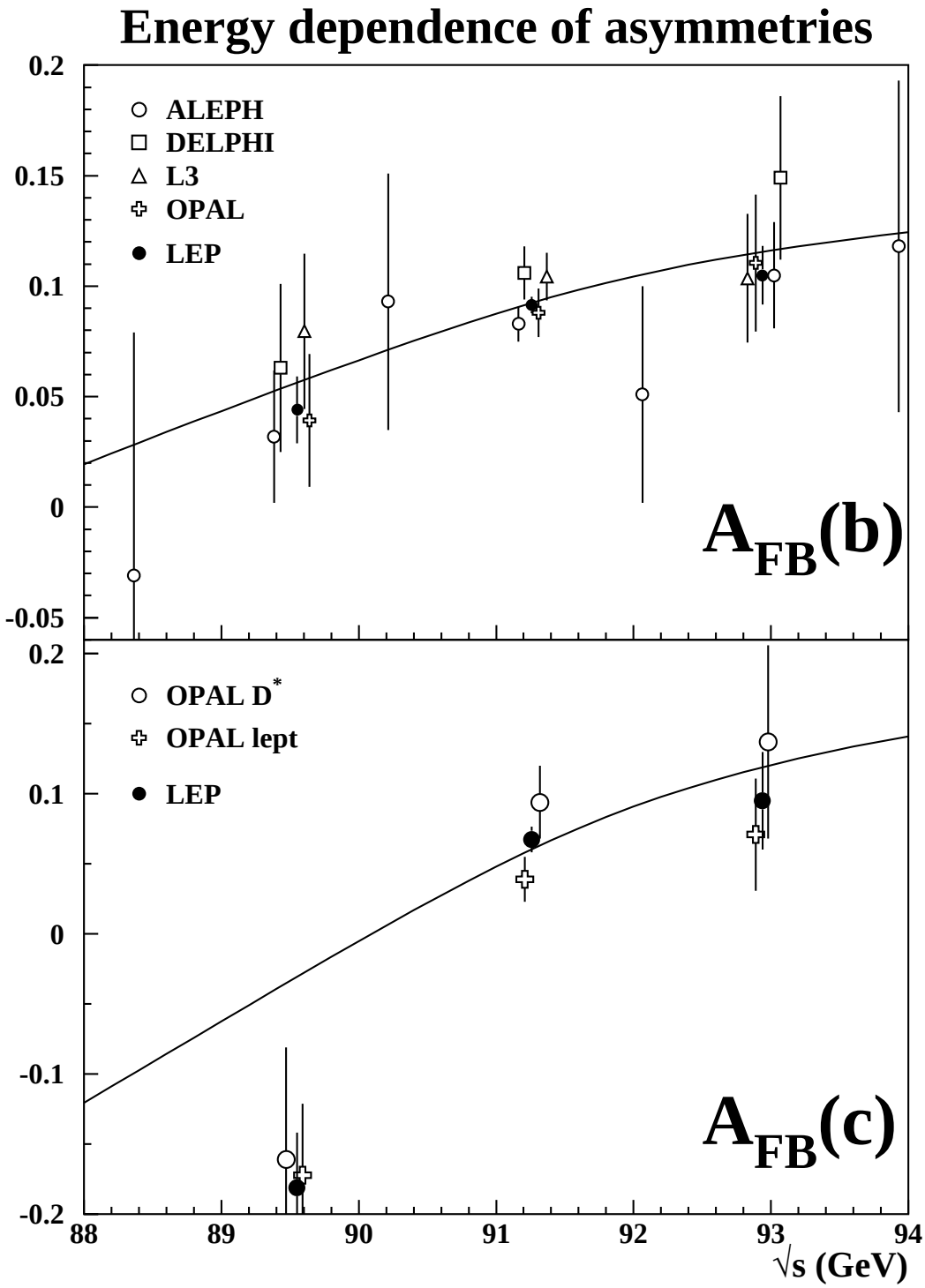

Figure 9: Energy dependence of heavy flavor asymmetries measured at LEP.

3 Lifetimes of b Hadrons

In the naive spectator model, the lifetimes of the B_d^0, B^-, B_s^0, and Λ_b hadrons are equal, depending only on the weak decay of the b quark. This expectation is modified by processes including W exchange and annihilation, and final state quark interference. From a $1/M_b$ expansion,[20] it is possible to predict the ratios of b-hadron lifetimes:

$$\begin{aligned} \tau(B^-)/\tau(B_d^0) &\approx 1.05, \\ \tau(B_s^0)/\tau(B_d^0) &\approx 1, \\ \tau(\Lambda_b)/\tau(B_d^0) &\approx 0.9. \end{aligned}$$

The measurements of the average lifetime of a particular b hadron all follow roughly the same prescription:

- Select a sample of candidate events by (semi)exclusive reconstruction of particular decay modes of the desired hadron.
- Reconstruct the primary and secondary vertices, and estimate the b-hadron decay length, L.
- Estimate the boost of the b hadron in order to convert the decay length into a proper time, $t = L/\beta\gamma c = LM_B/cp_B$, where M_B and p_B are the b-hadron mass and momentum, respectively.
- Perform an event-by-event likelihood fit to the distribution of proper times with the average lifetime as a free parameter.

The method for measuring the B_s^0 lifetime is presented first, which introduces many of the features common to all the lifetime analyses. This will be followed by brief descriptions of the Λ_b, B_d^0, and B^+ measurements.

3.1 B_s^0 Lifetime

ALEPH,[21] DELPHI,[22] and OPAL[23] have measured the B_s^0 lifetime using the following semileptonic decay chains:[†]

$$\begin{array}{lll} B_s^0 \to D_s^- \ell^+ \nu X & & B_s^0 \to D_s^- \ell^+ \nu X \\ \quad \hookrightarrow \phi\pi^- & & \quad \hookrightarrow K^{\star 0} K^- \\ \quad\quad \hookrightarrow K^+K^- & & \quad\quad \hookrightarrow K^+\pi^-. \end{array}$$

[†] In general, charge-conjugate decay chains are implied throughout this paper.

These offer a reasonable branching ratio and good signal to background, and so are suitable for a lifetime analysis. A schematic picture of such a decay is shown in Fig. 10. The D_s is reconstructed from three charged tracks, the K^+, K^-, and π^-

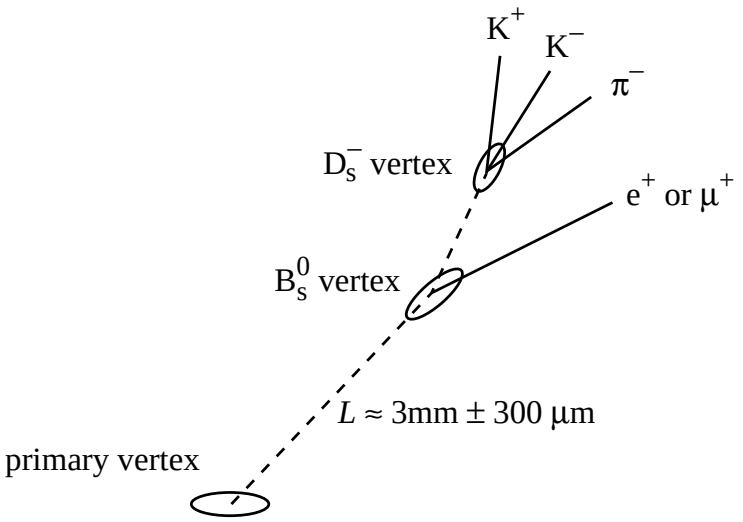

Figure 10: Schematic B_s^0 decay.

candidates. These tracks may be required to pass requirements on dE/dx in order to improve the K/π separation, to form a good vertex, and to satisfy kinematic requirements analogous to those imposed on the $D^\star$ decay products (see Sec. 2.4). The D_s candidate is then combined with an electron or muon candidate, and cuts are applied to the lepton p and p_T, and/or to the mass of the $D_s\ell$ combination. The resulting numbers of events and the background fractions are given in Table 2, and an example of the signal is given in Fig. 11. The B_s^0 decay length, L, is typically 3 mm. It is estimated by the distance from the primary to the B_s^0 vertex,[21,23] or to the D_s vertex,[22] with a typical resolution of 300 μm. The momentum of the B_s^0 candidate is estimated from the momentum of the $D_s\ell$ system, $p_{D\ell}$, with input from Monte Carlo simulations to give the distribution of possible boosts. The neutrino energy can be used to improve this estimate.[21]

The likelihood for event i, used to fit for the average lifetime, τ, can in general be written as:

$$\mathcal{L}^i = \mathcal{E}(t^i, \tau) \otimes \mathcal{G}(t^i, s\sigma_t^i) \otimes \mathcal{B}(p^i_{D\ell}), \tag{9}$$

where $\mathcal{E}$ is the distribution for an exponential decay with average lifetime τ, con-

	ALEPH	DELPHI	OPAL
Number of events	35 ± 7	37 ± 8	55 ± 10
Background fraction	0.25	0.30	0.35

Table 2: Sample sizes and purities for the semileptonic B_s^0 lifetime analyses.

voluted with a Gaussian distribution, $\mathcal{G}$, and with the expected distribution, $\mathcal{B}$, of the B_s^0 momentum given $p^i_{D\ell}$. The Gaussian has mean zero and width $s\sigma^i_t$, where σ^i_t is the error on the proper time, evaluated for each event, and s is an optional global scale factor to take into account wrongly estimated resolution effects. The fit result for the OPAL sample is shown in Fig. 12.

The backgrounds are mostly from random combinations of tracks and are parametrized from side-bands in the D_s mass distribution and/or from wrong sign $D_s\ell$ combinations. Less than 10% of the background arises from other B meson decays, such as $B \to D_s^+ \overline{D} X, \overline{D} \to \ell^- \nu X$, or $B \to D_s^- K \ell^+ \nu X$. These backgrounds with lifetimes are either parametrized by an additional term in the likelihood function or simply taken into account by assigning an additional systematic error. The dominant systematic errors in the measurement arise from the descriptions of the background and the boost estimate, and also from any possible bias in the fit which is assessed using Monte Carlo simulation.

The ALEPH Collaboration has also presented a result using the general decay mode $B_s^0 \to D_s^- h X$, where h represents any hadron, usually a pion.[24] The method is very similar to that using the $D_s\ell$ decay mode, with higher statistics, but more combinatorial background. The dominant systematic errors in this method arise from understanding the relative rates of candidate events from $Z \to c\overline{c}$ events compared with $b \to B_s^0 \to D_s^-$ events. DELPHI has gone one step further and presented an analysis based on inclusive $D_s \to \phi\pi$ events, where the large combinatorial background leads to the dominant error.[22]

All the B_s^0 lifetime measurements are summarized in Fig. 13. Here, the results of measurements by the CDF Collaboration are also included.[25] These are of similar precision to the measurements of the LEP Collaborations. The world averages take into account common sources of systematic uncertainty.[26]

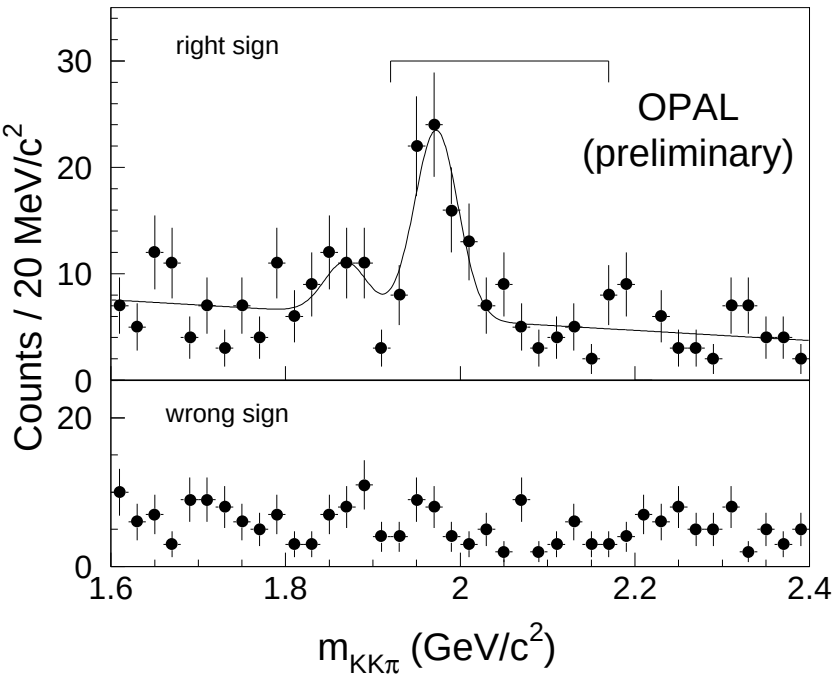

Figure 11: The OPAL D_s signal used in the B_s^0 lifetime analysis.

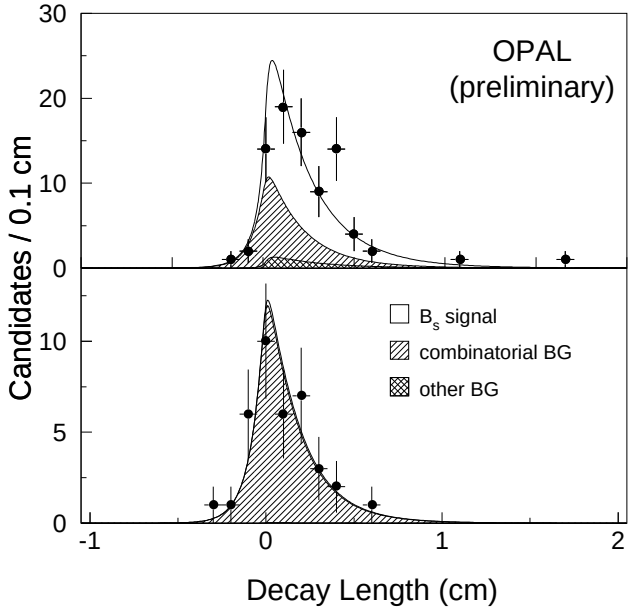

Figure 12: The decay length distribution of the selected OPAL B_s^0 events.

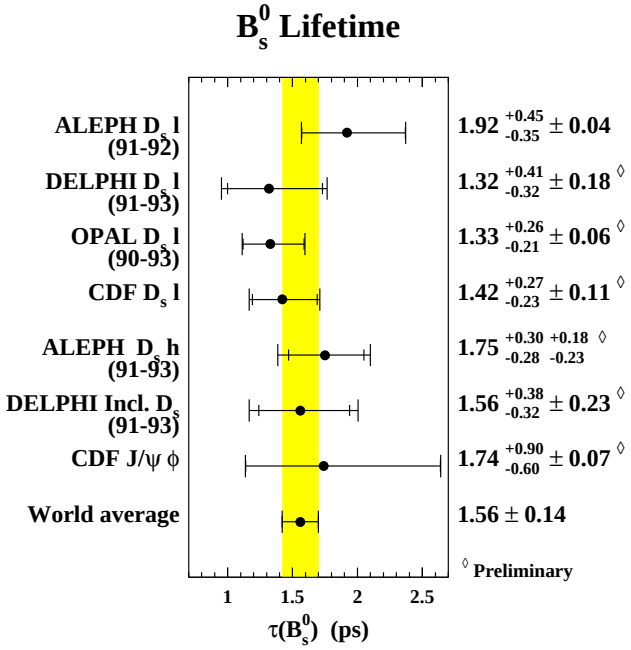

Figure 13: Measurements of the B_s^0 lifetime.

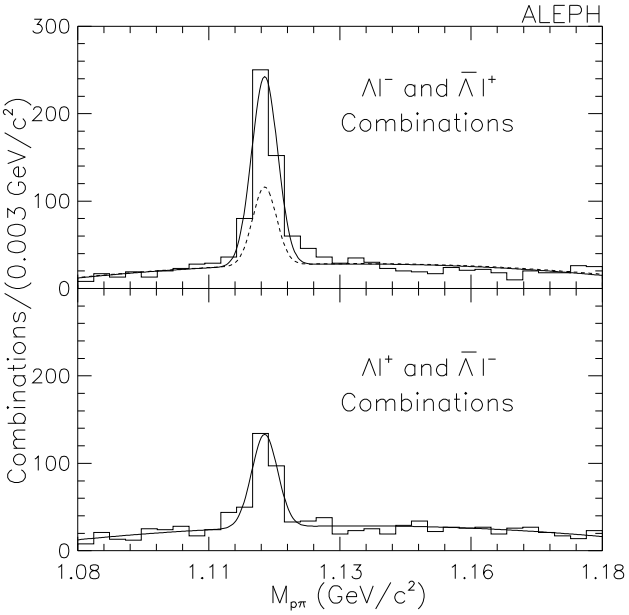

Figure 14: The $p\pi^-$ invariant mass distribution of ALEPH $\Lambda\ell^-$ and $\Lambda\ell^+$ combinations. The dashed curve represents the background level in the right sign sample estimated from the wrong sign sample after correction.

3.2 Lifetimes of b Baryons

Several methods have been used to measure the lifetimes of b baryons. A sample of Λ_b events can be selected from the decay:

$$\begin{aligned} \Lambda_b &\rightarrow \Lambda_c^+ \ell^- \bar{\nu} X \\ &\hookrightarrow \mathrm{pK}^- \pi^+. \end{aligned}$$

This is analyzed in just the same way as $B_s^0 \rightarrow D_s^- \ell^+ \nu X$. The choice of p, K, and π candidates can be improved using dE/dx requirements, with cuts on the mass of the $\Lambda_c \ell$ system to clean up the sample. The Λ_b boost is estimated from the momentum of the $\Lambda_c \ell$ system. Results have been presented by ALEPH[27] and DELPHI[28] using this technique.

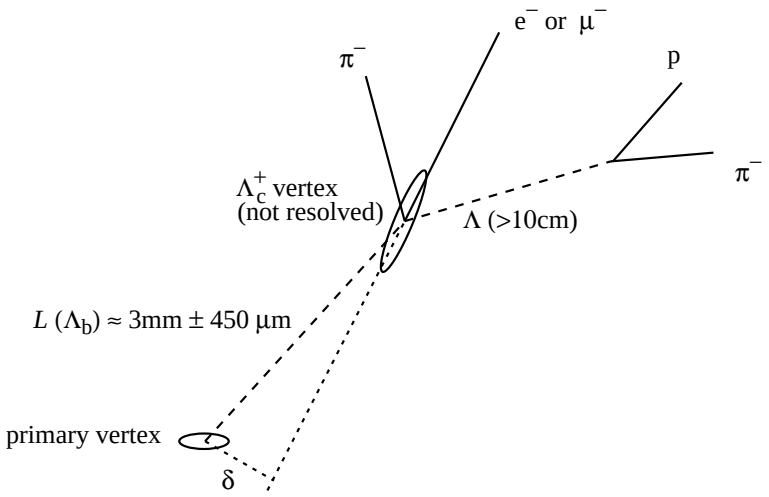

Figure 15: A schematic Λ_b decay.

A final state Λ associated with a charged lepton is a more general b-baryon tag, from decays such as:

$$\begin{aligned} \Lambda_b &\rightarrow \Lambda_c^+ \ell^- \bar{\nu} X \\ &\hookrightarrow \Lambda X \\ &\hookrightarrow \mathrm{p}\pi^- \end{aligned} \qquad\qquad \begin{aligned} \Xi_b^0 &\rightarrow \Xi_c^+ \ell^- \bar{\nu} X \\ &\hookrightarrow \Lambda X \\ &\hookrightarrow \mathrm{p}\pi^-. \end{aligned}$$

A Λ associated with a negative lepton is consistent with coming from a b-baryon decay.[‡] Wrong sign combinations, i.e., $\Lambda\ell^+$, give an estimate of the background coming from a genuine fragmentation Λ wrongly associated with a lepton or associated with a fake lepton candidate. An example is shown in Fig. 14. The side-bands of the Λ mass plot also give an estimate of the combinatorial background in the Λ signal. Backgrounds with lifetime content from physics processes are small.

A schematic event picture is shown in Fig. 15. The Λ often flies tens of centimeters before decaying, so that the resolution of the decay length varies strongly event-by-event. OPAL[29] reconstructs the Λ_b vertex from the $\Lambda\ell$ only, with an average resolution of about 450 μm. DELPHI[28] requires an additional hadron to be associated to the vertex, which helps to improve the resolution to typically 300 μm. A likelihood fit to the decay length distribution of right and wrong sign events (and to side-band events[28]) gives a measurement of the Λ_b lifetime. The dominant errors come from the unknown Λ_b polarization (which affects the distribution of the decay products), from the estimate of the boost and from the modeling of backgrounds.

The $\Lambda\ell$ samples have also been used to select leptons from a b-baryon decay to be used in an impact parameter analysis by ALEPH[30] and OPAL.[29] The lepton impact parameter, δ, is defined as the distance of closest approach of the lepton track to the primary vertex, signed according to whether the lepton intersects the accompanying jet downstream (positive) or upstream of the primary vertex. This is indicated in Fig. 15. A fit to the impact parameter distribution is made. The particle decays are modeled by Monte Carlo simulation using the resolution measured directly from the data. The contribution of background is again controlled by simultaneously fitting the wrong sign sample. The fit to the ALEPH sample is shown in Fig. 16. The Λ_b polarization is again a major source of uncertainty. The method is also sensitive to understanding the lepton identification schemes and to the modeling of background. The large statistical correlation between the OPAL decay length and impact parameter measurements has been taken into account to produce the combined OPAL number.

DELPHI has in addition attempted a more general muon-proton measurement of the b-baryon lifetime.[28] A proton sample is selected using the RICH detector,

[‡]It is expected that more Λ_b than Ξ_b^0 or Ξ_b^+ are produced, and from now on, the symbol Λ_b will also be used to denote the general b baryon.

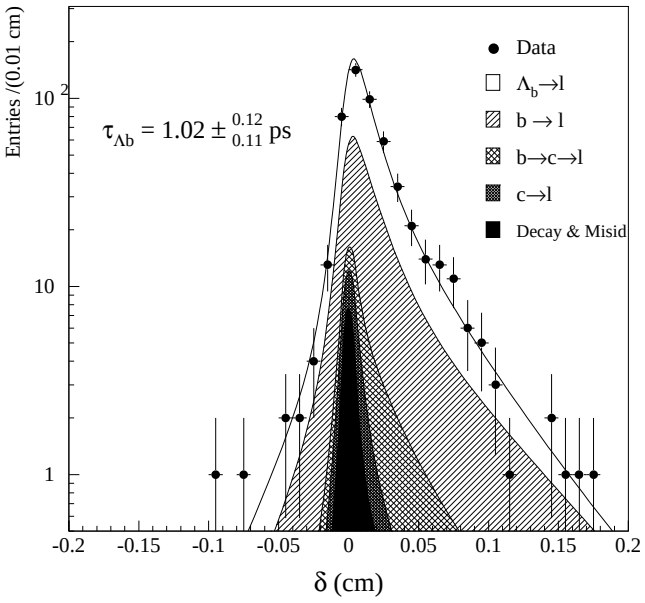

Figure 16: Impact parameter distribution of the selected ALEPH $\Lambda\ell^-$ candidates. The fit result is indicated by the curve.

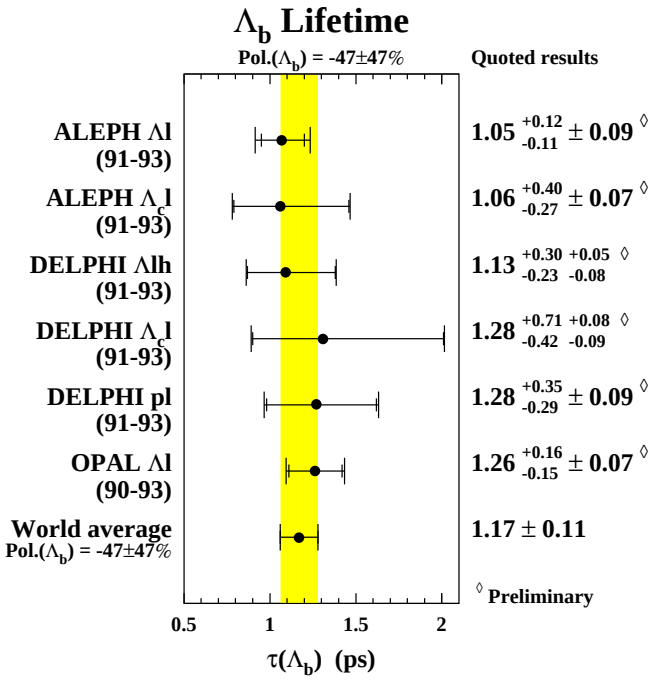

Figure 17: Measurements of the Λ_b lifetime.

and μp correlations are used in a similar way to $\Lambda\ell$ correlations above. The background is controlled by using tagged kaon or pion samples.

A summary of measurements of the b-baryon lifetimes is given in Fig. 17 (Ref. 31).

3.3 B_d^0 and B^+ Lifetimes

Conceptually, the most straightforward measurement of any b-hadron lifetime uses fully reconstructed decays, where the decay length and boost are unambiguously defined from data. The problem is the lack of statistics. In the case of B_d^0 and B^+ decays, ALEPH has used this technique, with the following decays:[32]

$$\begin{aligned} B^+ &\rightarrow \overline{D^0}\pi^+/\rho^+/{a_1}^+ \\ B^+ &\rightarrow \psi K^+ \\ B_d^0 &\rightarrow D^-\pi^+ \\ B_d^0 &\rightarrow D^{\star -}\pi^+ \, , \, D^{\star -} \rightarrow \overline{D^0}\pi^-. \end{aligned}$$

Here, ψ represents the J/ψ or the $\psi(2S)$ and is detected by its decays into e^+e^- or $\mu^+\mu^-$. The D^0 is identified in the modes $D^0 \rightarrow K^-\pi^+, K^-\pi^+\pi^0$, or $K^-\pi^+\rho^0$. Samples of 55 B^+ and 59 B_d^0 candidates were found, with background fractions of $(36 \pm 9)\%$ and $(22 \pm 9)\%$, respectively.

ALEPH, DELPHI, and OPAL have all measured the B_d^0 and B^+ lifetimes from samples of events with a D meson and a lepton in the final state:[33–35]

1. $D^0\ell^-$ where $D^0 \rightarrow K^-\pi^+$ with a $D^\star$ veto.
2. $D^+\ell^-$ where $D^+ \rightarrow K^-\pi^+\pi^+$ (only for the DELPHI and OPAL analyses).
3. $D^{\star +}\ell^-$ where $D^{\star +} \rightarrow D^0\pi^+$ and $D^0 \rightarrow K^-\pi^+(\pi^0)$ or $K^-\pi^+\pi^-\pi^+$.

The samples are cleaned up with the usual techniques: dE/dx for K/π separation, B and D vertex reconstruction, and decay kinematics consistent with the spin properties and a $D^{(\star)}\ell$ mass consistent with coming from a B meson. These samples can be used to measure the B_d^0 and B^+ lifetimes simultaneously because these two mesons constitute different fractions of each selection. The decays $B^+ \rightarrow D^0\ell^+X$ and $B_d^0 \rightarrow D^-\ell^+X$ contribute uniquely to categories 1 and 2, respectively. The branching ratios of charged and neutral $D^\star$ mesons then play a significant role:

$$\mathrm{Br}(D^\star(2010)^\pm \rightarrow D^0\pi^\pm) \;=\; 55\%$$

$$\begin{aligned} \mathrm{Br}(\mathrm{D}^\star(2010)^\pm \to \mathrm{D}^\pm(\pi^0 \text{ or } \gamma)) &= 45\% \\ \mathrm{Br}(\mathrm{D}^\star(2007)^0 \to \mathrm{D}^0(\pi^0 \text{ or } \gamma)) &= 100\%. \end{aligned}$$

This means that $\mathrm{B}^+ \to \mathrm{D}^{\star 0}\ell^+\mathrm{X}$ can only result in category 1 events, while $\mathrm{B}^0_\mathrm{d} \to \mathrm{D}^{\star -}\ell^+\mathrm{X}$ can contribute to all three samples. The picture is made slightly more complicated because the B mesons can decay to higher spin charmed mesons (denoted $\mathrm{D}^{\star\star}$), and the $\mathrm{D}^{\star\star 0}$ is sufficiently massive to decay to a charged or neutral $\mathrm{D}^{(\star)}$.

The fractions of B^0_d and B^+ mesons in each category, as a function of the decay proper time, depend on the average lifetimes of the B^0_d and B^+, the relative rates of B meson decay to different charm meson spin states, and the relative fractions of D and $\mathrm{D}^\star$ mesons in $\mathrm{D}^{\star\star}$ decays. Measured branching ratios and isospin arguments are used to derive the expected proportions of B^0_d and B^+ contributing to each sample. A combined fit for the B^0_d and B^+ lifetimes can then be performed. The combinatorial background is controlled using side-bands in the D mass distributions, and backgrounds with lifetime content from other physics processes are expected to contribute less than 5% of the events. The dominant systematic errors come from the modeling of the combinatorial background, and from the lack of knowledge of the $\mathrm{D}^\star$ fraction in $\mathrm{D}^{\star\star}$ decays.

The measurements of the B^0_d and B^+ lifetimes are given in Fig. 18. A result from DELPHI using inclusive secondary vertices with a well-defined charge[36] and results from CDF[37,38] are also shown. When the two lifetimes are measured simultaneously, many of the errors cancel in the ratio, which is shown in Fig. 19.

3.4 Summary of Lifetime Measurements

The world average lifetimes of the accessible b hadrons have been presented in the previous sections. By way of summary, ratios of these average values are given in Fig. 20, where they are compared with the theoretical expectation.[20] The sensitivity of the measurements is still too poor to draw any firm conclusions, although the Λ_b lifetime has a definite tendency to be lower than the B meson lifetimes. These lifetime measurements are all statistics limited. Many of the dominant systematic uncertainties are also statistics limited. In the future, the background properties will be better constrained by data, and input numbers which are at present a source of uncertainty are beginning to be measured at LEP. Examples of such measurements are given in Sec. 5.

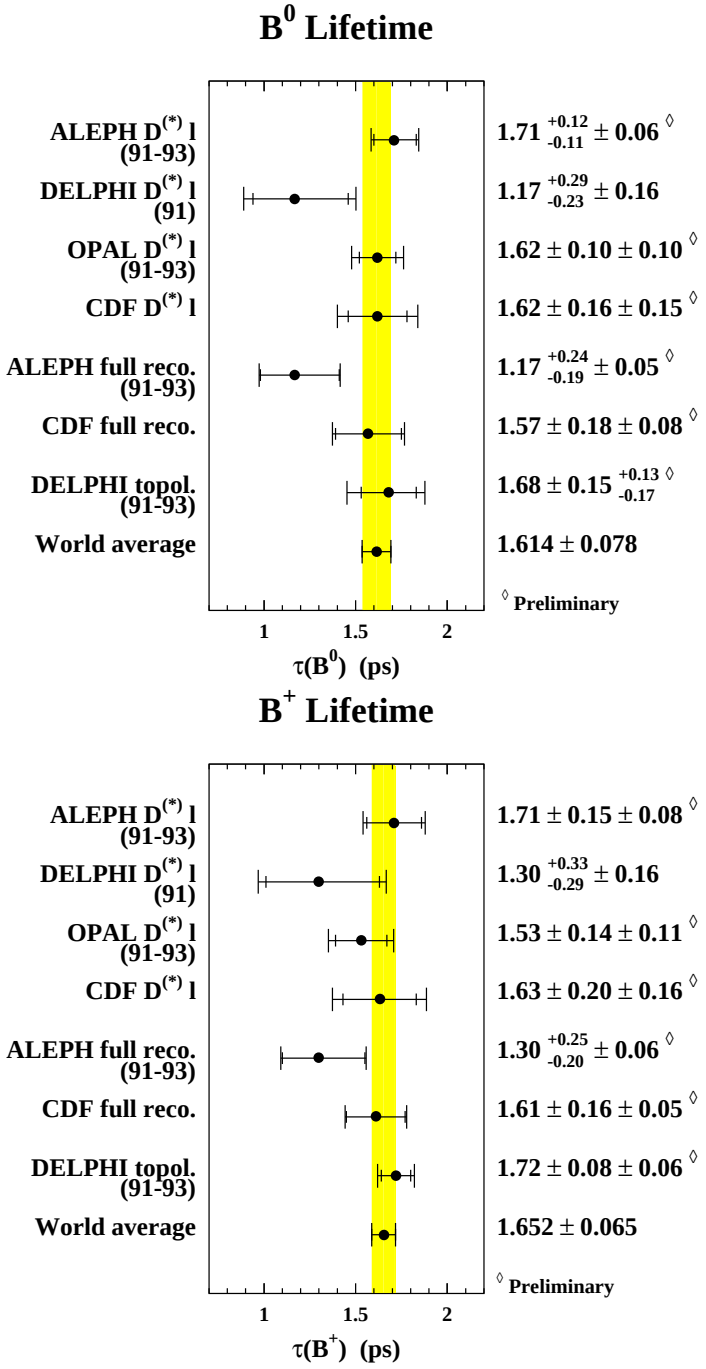

Figure 18: Measurements of the B^0_d and B^+ lifetimes.

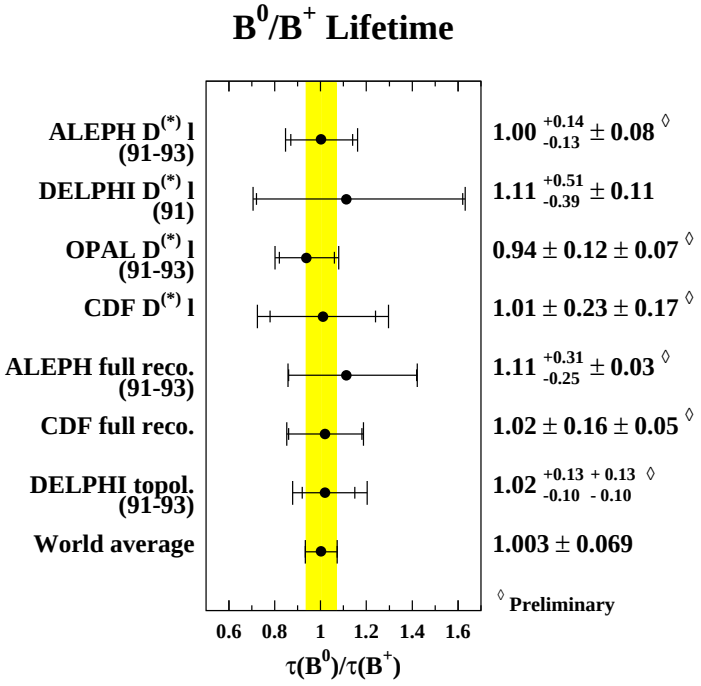

Figure 19: Measured ratios of B_d^0 and B^+ lifetimes.

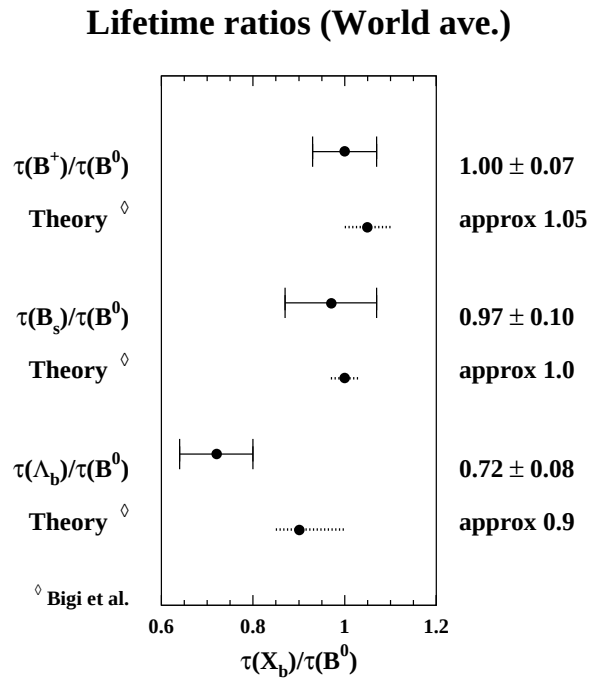

Figure 20: World average lifetime ratios compared with theory.

4 Time-Dependent B Mixing

The possibility that a neutral meson may transform into its own antiparticle was first recognized for neutral kaons and has since been observed for neutral B mesons. In the Standard Model, the relevant Feynman diagrams for this process are shown in Fig. 21. The dominant diagrams are those involving the top quark in the loops; the rate of mixing is proportional to $M^2_{\rm top}$ and to the product of CKM matrix elements $|V_{\rm tx}V^*_{\rm tb}|$, where x is d or s.[39]

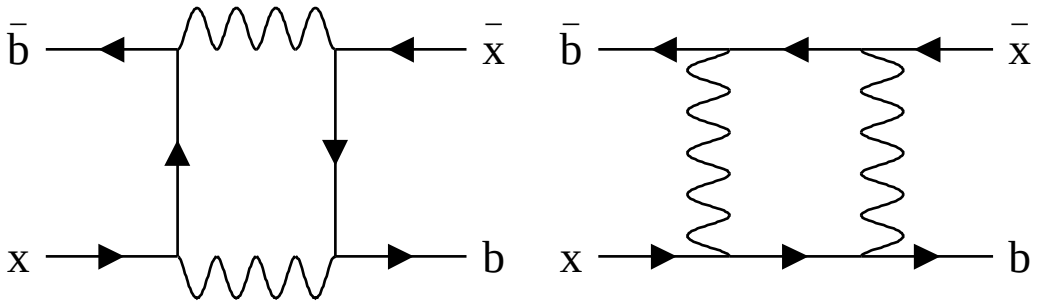

Figure 21: The box diagrams responsible for $\rm B^0\overline{B^0}$ mixing (x represents d or s).

The CP eigenstates, $\rm B_1$ and $\rm B_2$, are equivalent to the mass eigenstates if CP is conserved. They can be written as:

$$\rm B_1 = \frac{1}{\sqrt{2}}(B^0 + \overline{B^0}), \;\; B_2 = \frac{1}{\sqrt{2}}(B^0 - \overline{B^0}). \tag{10}$$

Similarly, the flavor eigenstates can be written in terms of the mass eigenstates. If a $\rm B^0$ is produced at the proper time $t = 0$, the probabilities for having a $\rm B^0$ or $\rm \overline{B^0}$ at proper time t are given by the respective amplitudes squared. The time dependence of the amplitudes of the mass eigenstates is given by the Schrödinger equation. The resulting probabilities are:

$$\mathcal{P}(\rm B^0, t) = \frac{1}{2\tau_B} e^{-t/\tau_B}(1 + \cos\Delta m t), \tag{11}$$

$$\mathcal{P}(\rm \overline{B^0}, t) = \frac{1}{2\tau_B} e^{-t/\tau_B}(1 - \cos\Delta m t), \tag{12}$$

where the mass difference is $\Delta m \equiv m_1 - m_2$, and $\tau_{\rm B} = 1/\Gamma$ is the average lifetime

of the B^0 and $\overline{B^0}$.[§] The number of observed B^0 and $\overline{B^0}$ decays oscillates as a function of proper time, within the usual exponential decay. The rate of mixing is often discussed in terms of $x = \Delta m/\Gamma$, which is 2π times the number of oscillations per average lifetime.

The first observations of $B^0\overline{B^0}$ mixing were of the time-integrated probability that a produced B^0 decays as a $\overline{B^0}$, given by:

$$\chi \equiv \mathcal{P}(B^0 \text{ decays as } \overline{B^0}) = \frac{1}{2}\frac{x^2}{1+x^2}. \tag{13}$$

At LEP, the effective value of χ depends on the relative fractions of B_d^0 and B_s^0, denoted f_d and f_s, and the time-integrated mixing for these two neutral mesons, χ_d and χ_s, respectively:

$$\chi = f_d\chi_d + f_s\chi_s.$$

Results for χ are shown in Fig. 22. The effective fractions are different for lepton-jet-charge measurements and lepton–lepton measurements, and the jet-charge measurements were therefore not included in the LEP average.[40] Measurements from $p\overline{p}$ colliders are also given in this figure.

Experiments at LEP have been able to observe directly the time structure of the mixing phenomenon for B mesons for the first time. A measurement of time-dependent mixing might proceed as follows:

- Select a sample enriched in B_d^0 or B_s^0 mesons.
- Measure the B^0 decay length and boost to determine the proper time of the decay, $t = L/\beta\gamma c$.
- Identify the $B^0/\overline{B^0}$ flavor at production and decay.
- Perform a fit as a function of proper time for the ratio, R, or asymmetry, A, of the numbers of mixed and unmixed events, $N_{\rm mix}$ and $N_{\rm unmix}$, respectively:

$$\begin{aligned} R &= N_{\rm mix}/(N_{\rm mix}+N_{\rm unmix}) \\ A &= (N_{\rm unmix}-N_{\rm mix})/(N_{\rm mix}+N_{\rm unmix}). \end{aligned}$$

  This fit should take into account the probability of each event to be signal or background.

[§] Any difference in the widths Γ_1 and Γ_2, which would arise from common final states of B^0 and $\overline{B^0}$, have been neglected.

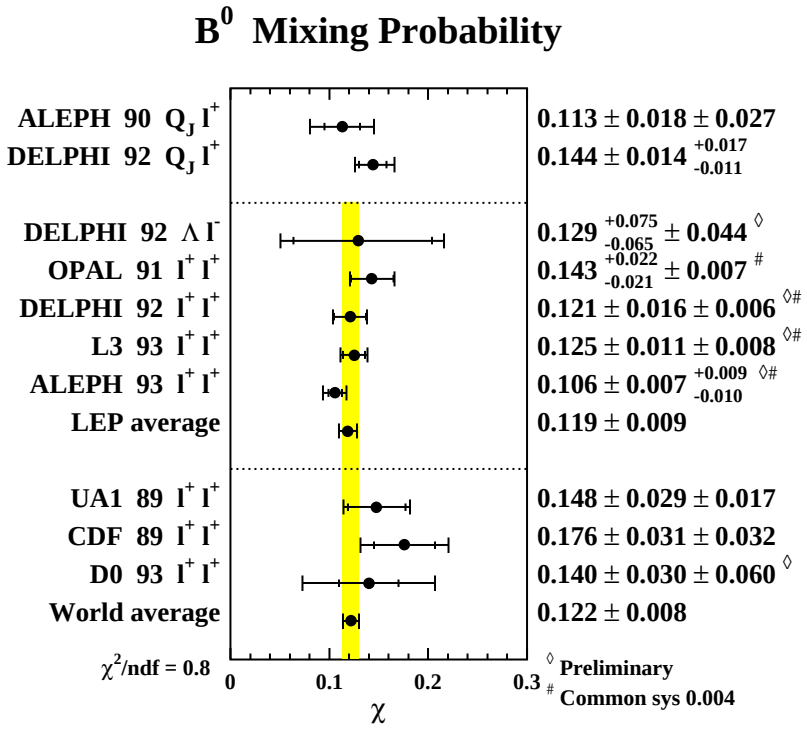

Figure 22: Measurements of time-integrated mixing.

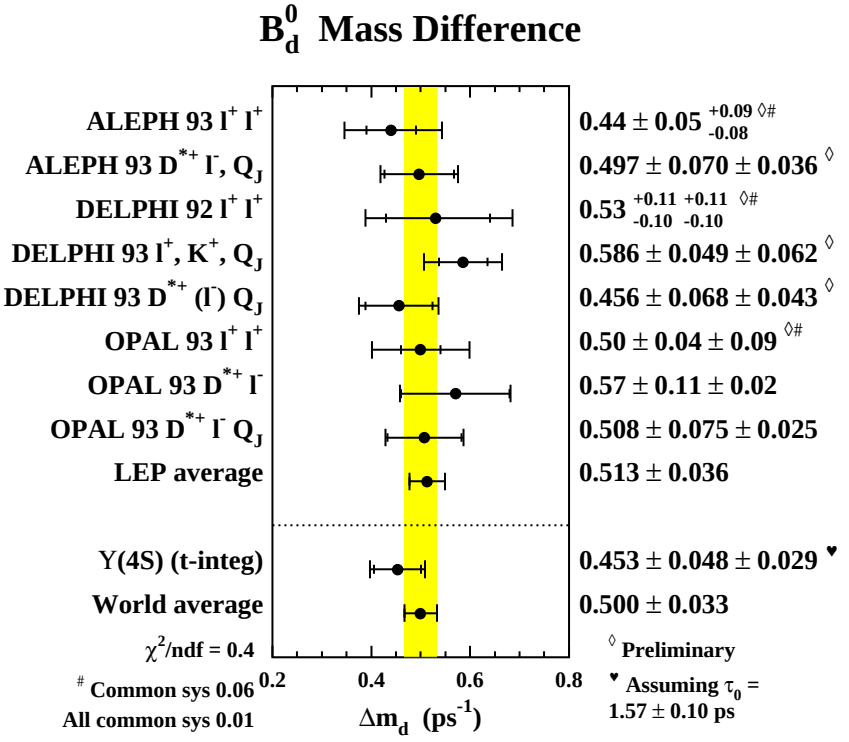

Figure 23: Measurements of $\Delta m_{\rm d}$.

This has many features in common with a lifetime analysis. Most of the decay modes considered for the lifetimes automatically provide the flavor of the decaying meson. The two extra ingredients are the need to know the production flavor and the extension of the fit to include the expected oscillatory behavior.

4.1 Measurements of $\Delta m_{\rm d}$

The results of a Monte Carlo study for $\rm B^0_d$ mixing with a $\rm D^\star$ tag are shown in Fig. 24. This serves to illustrate how a mixing signal is degraded by detector resolution, incorrect flavor tagging, and background.

Many analyses to measure $\Delta m_{\rm d}$ have been presented: events with a $\rm D^\star$ meson and a lepton in the same jet have been used by OPAL[41] to provide a $\rm B^0_d$–rich event sample where the flavor of the $\rm B^0_d$ at decay is known from the tag. The production state of the $\rm B^0_d$ is inferred from a jet-charge measure. Similar analyses have employed a $\rm D^\star$ meson tag opposite a lepton[42,43] or opposite a jet-charge measure.[42,44,45] Variations on the theme include measurements of $\Delta m_{\rm d}$ from leptons opposite leptons[46,47] and leptons or charged kaons opposite leptons, charged kaons or a jet-charge measure,[48] where the lepton or kaon is included in a reconstructed secondary vertex.

The general jet charge, $Q_{\rm jet}$, is defined in Eq. 7 but the exact choice of jet-charge measure is tuned for each analysis. This is illustrated by the $\rm D^\star\ell$ opposite jet-charge measurement of $\Delta m_{\rm d}$.[41] Fragmentation tracks, in the same hemisphere as the $\rm B^0_d$ tag, give information about whether a b or $\overline{\rm b}$ quark was originally produced in this hemisphere. A value of $\kappa = 0$ is chosen for all the tracks in this hemisphere, so that the net contribution of tracks from the $\rm B^0_d$ is identically zero, and the measure is insensitive to whether this is a mixed or unmixed event. Since b quarks in Z decays are produced in $\rm b\overline{b}$ pairs, the tracks in the opposite hemisphere also carry information about the flavor of the $\rm B^0_d$ at production. For the opposite hemisphere, a value of $\kappa = 1$ is found to give improved charge tagging. Most of the information comes from the opposite hemisphere, and the combined jet-charge measure used in the analysis is given by:

$$Q_{\rm tag} = Q^{\rm same}_{\rm jet}(\kappa = 0) - 10 Q^{\rm opp}_{\rm jet}(\kappa = 1). \qquad (14)$$

The fraction of events where the jet-charge gives the wrong production flavor is a free parameter in the fit for the fraction of "like-sign" events as a function of

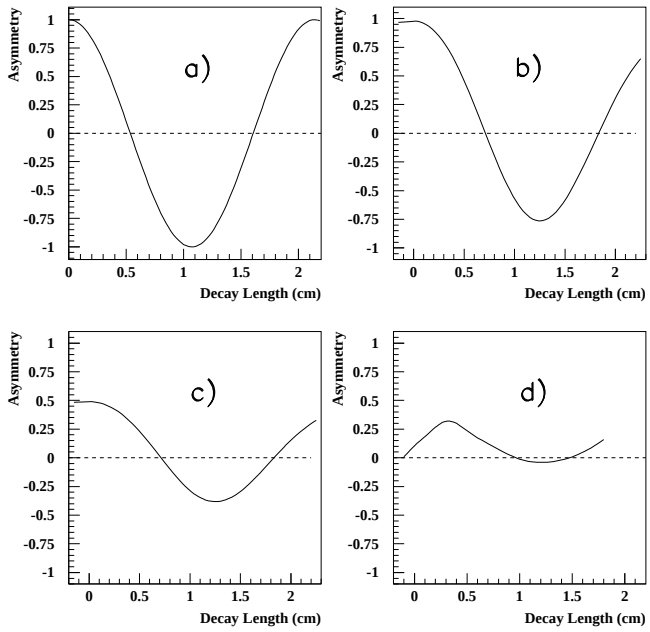

Figure 24: The asymmetry, $A(L)$, between unmixed and mixed events for a Monte Carlo B^0_d mixing experiment, as a function (a) of the true B^0_d decay length with fixed B^0_d momentum, (b) with realistic resolution and momentum spread, (c) with incorrect flavor tagging for 25% of events, and (d) including backgrounds.

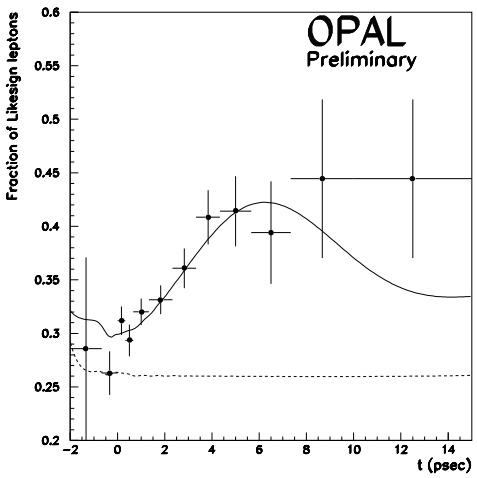

Figure 25: The fraction of like-sign leptons as a function of proper time, $R(t)$. The solid curve represents the expectation with $\Delta m_d = 0.5$ ps^{-1} and $\Delta m_s = 10$ ps^{-1}. The dashed curve represents the prediction with no B^0_d mixing.

proper time, and is measured to be 0.26 ± 0.03. This is in good agreement with the expectation from Monte Carlo simulation.

The measurements of $\Delta m_{\rm d}$ are summarized in Fig. 23. The time-integrated mixing observed in $\Upsilon(4S)$ decays has also been expressed in terms of $\Delta m_{\rm d}$.[40] The world average value for $\Delta m_{\rm d}$ in units of mass, and the equivalent value of $x_{\rm d}$, using the world average $\rm B^0_d$ lifetime, are:

$$\begin{aligned} \Delta m_{\rm d} &= (3.29 \pm 0.22) \times 10^{-4} {\rm eV}/c^2 \\ x_{\rm d} &= 0.79 \pm 0.07. \end{aligned}$$

4.2 Limits on $\Delta m_{\rm s}$

The lepton-tagged samples include contributions from all b-hadron semileptonic decays. A fit to the mixed fraction with two frequency components allows an investigation of $\Delta m_{\rm d}$ and $\Delta m_{\rm s}$. This has been attempted with samples of events with two leptons[46,47] and with a lepton opposite a jet-charge measure.[49] An example from OPAL[47] comparing the expectation for a given $\Delta m_{\rm s}$ with data is shown in Fig. 25. The negative log-likelihood difference from the minimum, $\Delta\mathcal{L}$, as a function of $\Delta m_{\rm d}$ and $\Delta m_{\rm s}$ from the ALEPH lepton-lepton analysis,[46] is shown in Fig. 26. It is not possible to distinguish between high values of $\Delta m_{\rm s}$, because the high-frequency oscillations are not resolvable. In other words, all high frequencies above some value are equally likely. However, it is possible to set a limit excluding low values of $\Delta m_{\rm s}$.

Limits have been set in as many ways as there are analyses, and all are to some extent based on a Monte Carlo technique. For the ALEPH lepton-lepton analysis, a set of Monte Carlo experiments with the same number of events as in the data sample are made for each value of $\Delta m_{\rm s}$ to be considered. For each experiment, $\Delta\mathcal{L}_0$ is defined as the value of $\Delta\mathcal{L}$ at the true value of $\Delta m_{\rm s}$. For each value of $\Delta m_{\rm s}$ considered, 5% of Monte Carlo experiments have $\Delta\mathcal{L}_0$ above some value, $\Delta\mathcal{L}_0(5\%)$, which would ideally be 1.92, and in practice, is close to this value. The log-likelihood function for the real data then allows the exclusion at 95% C.L. of values of $\Delta m_{\rm s}$ at the point where $\Delta\mathcal{L}_0 = \Delta\mathcal{L}_0(5\%)$. In order to take into account the effect of systematic uncertainties, this Monte Carlo approach is extended to modify the limit contour[46] (illustrated in Fig. 27). A similar approach is used by OPAL[47] to modify the log-likelihood curve as a function of $\Delta m_{\rm s}$. The ALEPH lepton-jet-charge analysis[49] is based on the variable $\Delta\mathcal{L}_\infty$, defined as the

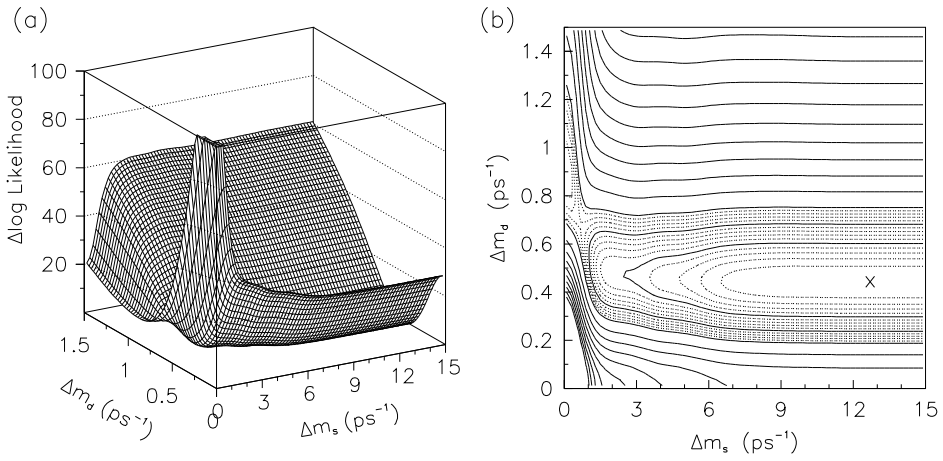

Figure 26: The distribution of $\Delta\mathcal{L}$ for the ALEPH lepton-lepton analysis (a) as a function of $\Delta m_{\rm s}$ and $\Delta m_{\rm d}$, shown as a surface plot; (b) the same shown as a contour plot—the dotted contours are spaced by one unit in log-likelihood, the solid contours are spaced by five units, and the cross shows the minimum.

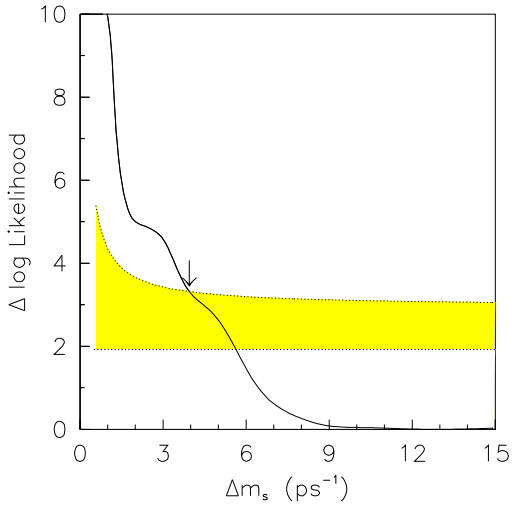

Figure 27: The $\Delta\mathcal{L}$ limit curve for the ALEPH lepton-lepton analysis. The upper and lower edges of the shaded region show the limit curve with and without systematic errors, respectively. The resulting limit is indicated by the arrow.

difference between the log-likelihood at the true value of $\Delta m_{\rm s}$ and as $\Delta m_{\rm s} \to \infty$. The resulting 95% confidence limits for these three analyses[46,47,49] are $\Delta m_{\rm s} > 3.9$, 1.3, and 6 ps^{-1}, respectively. The effective LEP limit is therefore, from the ALEPH lepton-jet-charge analysis,

$$\Delta m_{\rm s} > 6 {\rm ps}^{-1}.$$

This assumes a $\rm B_s^0$ fraction of $f_{\rm s} = 0.12 \pm 0.04$. If one also takes $\tau(\rm B_s^0) = 1.56 \pm 0.14$ ps and reduces the central value by one standard deviation, this limit corresponds to:

$$x_{\rm s} > 8.5.$$

The ratio of $\Delta m_{\rm s}$ to $\Delta m_{\rm d}$ in the Standard Model is:[40]

$$\frac{\Delta m_{\rm s}}{\Delta m_{\rm d}} = (1.2 \pm 0.1) \left| \frac{V_{\rm ts}}{V_{\rm td}} \right|^2 . \tag{15}$$

Combining the LEP $\Delta m_{\rm s}$ limit with the measured value of $\Delta m_{\rm d}$ gives:

$$\frac{\Delta m_{\rm s}}{\Delta m_{\rm d}} > 11.3, \quad \left| \frac{V_{\rm ts}}{V_{\rm td}} \right| > 3.0.$$

This constraint on $|V_{\rm ts}/V_{\rm td}|$ compares with a limit from the unitarity[40,50] of 2.9.

5 Further Properties of Heavy Hadrons

Several of the measurements presented so far have sources of systematic uncertainty which are themselves amenable to study at LEP. This section gives a few further examples of heavy quark measurements, some of which have a direct bearing on these systematic uncertainties already mentioned.

5.1 $\Lambda_{\rm b}$ Polarization

The quarks produced in Z decay are polarized. This polarization is expected to be preserved for b baryons, where in the heavy quark limit, the b-quark spin is decoupled from the light quark system. The $\Lambda_{\rm b}$ polarization strongly affects the momentum spectrum of the leptons produced in its semileptonic decay. The ALEPH Collaboration has attempted to measure $\Lambda_{\rm b}$ polarization[51] using the decay chain

$$\begin{aligned} \Lambda_{\rm b} \quad &\to \quad \Lambda_{\rm c}{}^+ \ell^- \bar{\nu} X \\ &\qquad \hookrightarrow \Lambda \pi^+ X, \end{aligned}$$

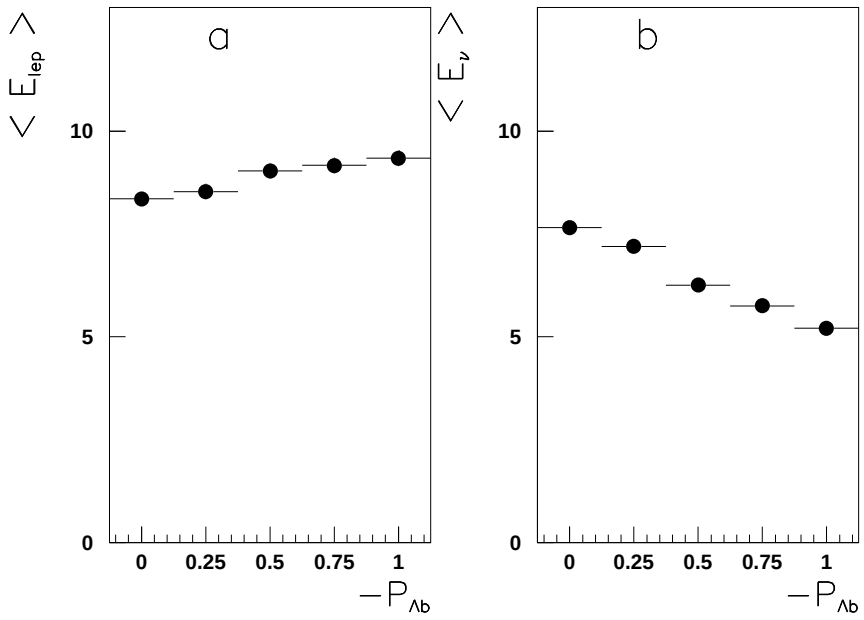

Figure 28: (a) Monte Carlo simulation of the mean charged lepton energy, and (b) the mean neutrino energy in the laboratory frame, as a function of Λ_b polarization.

where the ℓ^-, $\Lambda \to p\pi^-$, and π^+ are identified. The neutrino energy is reconstructed from the missing energy flow in the event. The expected mean energy for the charged lepton and neutrino are shown in Fig. 28 as a fuction of the Λ_b polarization. As would be expected from these distributions, the ratio $y = \langle E_\ell \rangle / \langle E_\nu \rangle$ is a sensitive variable for measuring the Λ_b polarization. Comparing the value of y observed in data to the value expected in Monte Carlo yields a measurement of the polarization:

$$\mathcal{P}_{\Lambda_b} = -0.30^{+0.32}_{-0.27} \pm 0.04.$$

5.2 Higher Spin States of D Mesons

The charm meson states with orbital momentum $L = 1$ are often called $D^{\star\star}$ or D_J. The predicted particles, one charged and one neutral for each spin state, and their allowed decay modes are:[52]

$$\begin{array}{lll}
(^3P_0) & D_0^\star(2360) \to D\pi & \Gamma \approx 200 \text{ MeV} \\
(^1P_1) & D_1(2430) \to D^\star\pi & \Gamma \approx 200 \text{ MeV} \\
(^3P_1) & D_1^\star(2430) \to D^\star\pi & \Gamma \approx 20 \text{ MeV} \\
(^3P_2) & D_2^\star(2460) \to D\pi, D^\star\pi & \Gamma \approx 30 \text{ MeV}.
\end{array}$$

	ALEPH	DELPHI	Average
$R_b^{\star\star}$	$0.159 \pm 0.048 \pm 0.031$	$0.17 \pm 0.06 \pm 0.03$	0.164 ± 0.043
$R_c^{\star\star}$	$0.084 \pm 0.024 \pm 0.023$	$0.11 \pm 0.03 \pm 0.02$	0.096 ± 0.033

Table 3: The fraction of $D^\star$ mesons coming from $D^{\star\star}$ decay in $b\overline{b}$ and $c\overline{c}$ events.

The degree of mixing between the two P_1 states is not known, but one is expected to be narrow and the other broad. Evidence for $D^{\star\star}$ states in hadronic Z decays has been reported by ALEPH[53] and DELPHI,[13] and specifically in semileptonic B decays by ALEPH,[54] DELPHI,[13] and OPAL.[55] The $D^{\star\star}$ signal is found by combining a D or $D^\star$ with an additional pion. An example is shown in Fig. 29. Lifetime information and x_E are used to distinguish $b\overline{b}$ and $c\overline{c}$ events. Denoting $R_b^{\star\star} = \Gamma(b \to D^{\star\star 0} X \to D^{\star +}\pi^- X)/\Gamma(b \to D^{\star +} X)$ and similarly $R_c^{\star\star}$ for $c\overline{c}$ events, the fractions of $D^\star$ mesons expected to come from $D^{\star\star}$ decay are given in Table 3. The observations made in semileptonic B decays are:

- ALEPH: $D_1 + (D^\star\pi)_{\rm NonResonant}$ contribute about 25% of $B \to D^{(\star)}\ell\nu X$.
- DELPHI: The ratio $D^{\star\star}\ell\nu/D^\star\ell\nu$ is about 20%.
- OPAL: $34 \pm 7\%$ of $B \to D^{(\star)}\ell\nu X$ are from narrow $D^{\star\star}$ states.

These observations reinforce the fact that a significant fraction of $D^{\star\star}$ mesons are produced in $c\overline{c}$ events and in B-meson decay.

5.3 Observations of $B^\star$ Mesons

The mass difference between $B^\star$ and B mesons, from the decay $B^\star \to B\gamma$, has been measured by the CLEO and CUSB Collaborations[50] to be 46.0 ± 0.6 MeV for B_d^0 and B^+, and 47.0 ± 2.6 MeV for B_s^0 mesons. For $B^\star$ mesons produced in Z decays, the photon is boosted, and the laboratory frame energy $E_{\rm lab}$ is $\lesssim 800$ MeV. The $B^\star$ rest frame energy, $E_{\rm rest}$, is given by:

$$E_{\rm rest} = E_{\rm lab}\gamma_B(1 - \beta_B \cos\theta), \tag{16}$$

where γ_B and β_B are the boost and velocity of the B meson, and θ is the angle between the B and the photon in the $B^\star$ rest frame. The laboratory energy can be measured from the energy deposited in the electromagnetic calorimeter,[56,57]

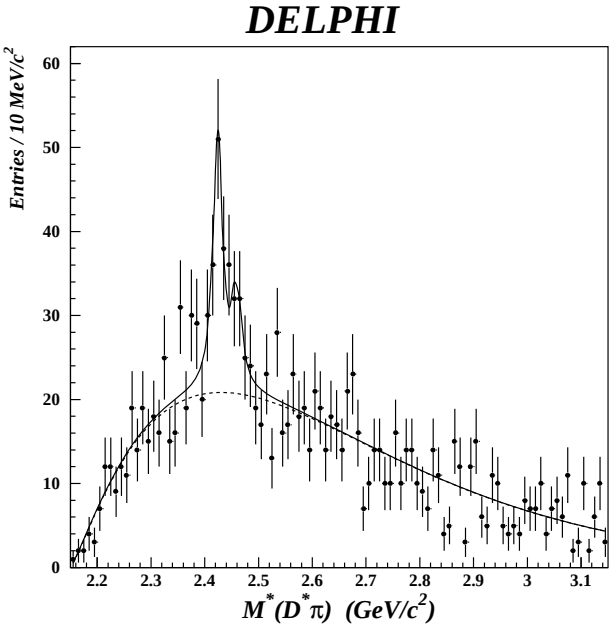

Figure 29: The invariant mass of $D^{\star+}\pi^-$ combinations from DELPHI, showing the background parametrization (dotted). The solid curve includes the signal.

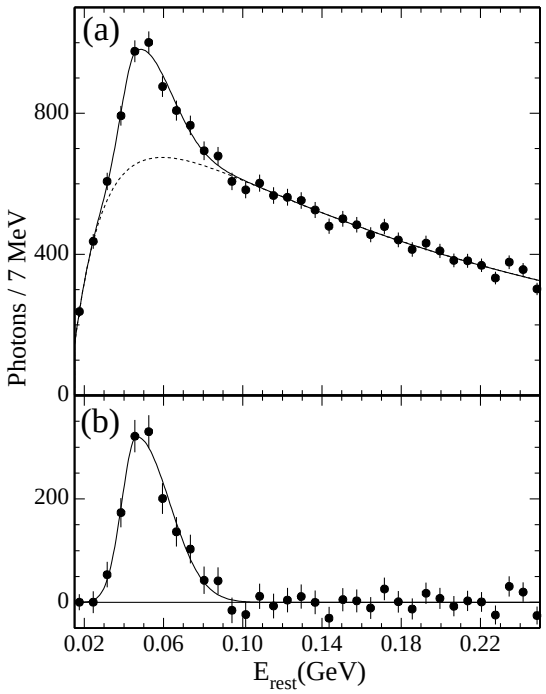

Figure 30: From L3, (a) the rest frame photon energy spectrum, and (b) the $B^\star$ signal after background subtraction.

	ALEPH	DELPHI	L3
ΔM (MeV)	$45.1 \pm 0.6 \pm 0.9$	$45.3 \pm 0.4 \pm 0.6$	
$B^\star/(B^\star + B)$	$0.800 \pm 0.040 \pm 0.062$	$0.73 \pm 0.04 \pm 0.06$	$0.77 \pm 0.07 \pm 0.10$
$D^\star/(D^\star + D)$	0.53 ± 0.16	0.45 ± 0.06	
$\sigma_L/(\sigma_L + \sigma_T)$	$0.32 \pm 0.09 \pm 0.08$	$0.33 \pm 0.07 \pm 0.07$	

Table 4: Results from $B^\star$ samples. ΔM denotes $M(B^\star) - M(B)$. The measured value of $V/(V+P)$ for charm mesons is also quoted for comparison.

or by reconstructing a converted photon in the tracking detectors.[56,58] The experiments select a $b\overline{b}$ enriched sample with a lifetime or lepton tag, and perform inclusive B reconstruction within jets to estimate the B boost. Preliminary measurements of $B^\star$ properties are given in Table 4. The expected fraction of vector mesons produced and the fraction of longitudinally polarized $B^\star$ mesons agree with the expectations of heavy quark effective theory: $V/(V+P) = 0.75$ and $\sigma_L/(\sigma_L + \sigma_T) = 0.33$. The latter is measured from the distribution of the angle of the photon with respect to the $B^\star$ flight direction in the $B^\star$ rest frame. For comparison, measurements of $V/(V+P)$ for charm mesons are also listed in Table 4. In this case, the result does not adhere to the naive spin counting expectation.

6 Outlook

LEP has already produced a rich harvest of b and c hadrons, and is still running at the Z pole. Although there is a large systematic component to the error, the measurement of R_b will improve with more data. Tagging algorithms can be refined, tighter cuts can be applied to optimize the total error in a trade-off between systematic and statistical uncertainties, and other measurements will help to reduce the systematic errors.

These comments apply to many other analyses. Not only are many of these measurements statistics limited, but as has been illustrated in the latter part of this review, their systematic errors are themselves statistics limited. We can look forward to increasingly stringent tests of the Standard Model and heavy quark theory at LEP.

Acknowledgments

It is a pleasure to thank the organizers for such an enjoyable Summer Institute. I would also like to thank my colleagues on the LEP experiments for their help in preparing this talk, especially Dave Charlton, Martin Jimack, Roger Jones, and Dale Koetke for their valuable comments on this manuscript.

References

[1] *Z Physics at LEP 1 - Volume 1*, edited by G. Altarelli, CERN 89-08, Sept. 1989.

[2] The LEP Electroweak Working Group and the LEP Collaborations: ALEPH, DELPHI, L3, OPAL, "Combined preliminary data on Z parameters from the LEP experiments and constraints on the Standard Model," CERN-PPE/94-187, and references therein.

[3] ALEPH Collaboration, D. Buskulic et al., Phys. Lett. B **313** 535 (1993).

[4] DELPHI Collaboration, "DELPHI results on electroweak physics with quarks," contributed to the *Glasgow Conference ICHEP94, Ref. GLS0301, DELPHI 94-111 PHYS 428.*¶

[5] OPAL Collaboration, "Measurement of $\Gamma_{b\overline{b}}/\Gamma_{had}$ using a double tagging method," CERN-PPE/94-106, submitted to Z. Phys. C.

[6] ALEPH Collaboration, D. Buskulic et al., Phys. Lett. B **313**, 549 (1993).

[7] L3 Collaboration, O. Adriani et al., Phys. Lett. B **307**, 237 (1993).

[8] ALEPH Collaboration, "Heavy flavour lepton," contribution for the *Summer 1994 Conferences: ALEPH 94-123, PHYSIC 94-107*;
"$B^0\overline{B^0}$ mixing and $b\overline{b}$ asymmetry from high p_t leptons," ALEPH 94-036; ALEPH Collaboration, D. Buskulic et al., Z. Phys. C **62**, 179 (1994).

[9] DELPHI Collaboration, "Measurement of R_b using microvertex and lepton double tags," Glasgow ICHEP94, Ref. GLS0229, DELPHI 94-91, PHYS 408.

[10] L3 Collaboration, "L3 results on A_{FB}^b, A_{FB}^c and χ," for the *Glasgow Conference,* L3 Note 1624;
"Measurement of the $B^0\overline{B^0}$ mixing parameter and the $Z \to b\overline{b}$ forward-backward asymmetry," CERN-PPE/94-89, submitted to Phys. Lett. B;
L3 Collaboration, O. Adriani et al., Phys. Lett. B **292**, 454 (1992);
"L3 results on R_b and $Br(b \to \ell)$," for the *Glasgow Conference,* L3 Note 1625;
"Measurement of R_b and $Br(b \to \ell X)$ from b-quark semi-leptonic decays," L3 Note 1449.

[11] OPAL Collaboration, "The forward-backward asymmetry of $e^+e^- \to Z \to b\overline{b}$ and $e^+e^- \to Z \to c\overline{c}$ from events tagged by a lepton," OPAL Physics Note PN118;
OPAL Collaboration, R. Akers et al., Z. Phys. C **60**, 199 (1993).

[12] DELPHI Collaboration, "Measurement of the forward-backward asymmetry of $e^+e^- \to Z \to b\overline{b}$ using prompt leptons and a microvertex tag," Glasgow ICHEP94, Ref. GLS0203, DELPHI 94-62, PHYS 383.

¶ "Glasgow" indicates the XXVII International Conference on High Energy Physics, Glasgow, July 20-27, 1994.

[13] DELPHI Collaboration, "Study of D, $D^{\star}$, and $D^{\star\star}$ production in Z hadronic decays," Glasgow ICHEP94, Ref. GLS0185, DELPHI 94-103, PHYS 420.

[14] OPAL Collaboration, "A measurement of the production of $D^{\star\pm}$ mesons on the Z resonance," OPAL Physics Note PN148.

[15] ALEPH Collaboration, "The forward-backward asymmetry for charm quarks at the Z pole," Glasgow, ICHEP94, Ref. GLS0562.

[16] DELPHI Collaboration, "Measurement of the forward-backward asymmetry of charm and bottom quarks at the Z pole using $D^{\star\pm}$ mesons," DELPHI 94-95, PHYS 412.

[17] OPAL Collaboration, "Updated measurement of the forward-backward asymmetry of $e^+e^- \to b\overline{b}$ and $e^+e^- \to c\overline{c}$ on and near the Z peak using $D^{\star\pm}$ mesons," OPAL Physics Note, PN125.

[18] ALEPH Collaboration, "A measurement of A_{FB}^{b} in lifetime tagged heavy flavour Z decays," CERN-PPE/94-84, submitted to Phys. Lett. B.

[19] OPAL Collaboration, "A measurement of the forward-backward asymmetry of $e^+e^- \to b\overline{b}$ using a jet charge algorithm and lifetime tagged events," OPAL Physics Note PN127.

[20] Bigi et al., "Nonleptonic decays of beauty hadrons: From phenomenology to theory," CERN-TH 7132/94.

[21] ALEPH Collaboration, "Measurement of the B_s^0 lifetime," CERN-PPE/93-214.

[22] DELPHI Collaboration, "Measurement of B_s^0 lifetime using D_s–lepton and inclusive D_s samples," Glasgow ICHEP94, Ref. GLS0233, DELPHI 94-116, PHYS 433.

[23] OPAL Collaboration, "An updated measurement of the B_s^0 lifetime," OPAL Physics Note PN150.

[24] ALEPH Collaboration, "Measurement of the B_s^0 lifetime with D_s + hadron events," Glasgow ICHEP94, Ref. GLS0578.

[25] CDF Collaboration, "Measurement of the B_s^0 meson lifetime at CDF," Glasgow ICHEP94, Ref. GLS0609.

[26] C. H. Shepherd-Themistocleous, "Review of B_s^0 lifetimes," presented at Glasgow.

[27] ALEPH Collaboration, "Λ_b lifetime measurement," Glasgow ICHEP94, Ref. GLS0596.

[28] DELPHI Collaboration, "Lifetime and production rate of beauty baryons from Z decays," Glasgow ICHEP94, Ref. GLS0162, DELPHI 94-117, PHYS 434.

[29] OPAL Collaboration, "Measurement of the average b-baryon lifetime," Glasgow ICHEP94, Ref. GLS0534, OPAL Physics Note PN146.

[30] ALEPH Collaboration, "A measurement of the b baryon lifetime," Glasgow ICHEP94, Ref. GLS0603.

[31] L. Moneta, "Review of b baryon lifetime measurements at LEP," presented at Glasgow.

[32] ALEPH Collaboration, "Measurement of the B^+ and B^0 lifetimes using exclusively reconstructed events," Glasgow ICHEP94, Ref. GLS0602.

[33] ALEPH Collaboration, "Measurement of the $\overline{B^0}$ and B^- meson lifetimes," Glasgow ICHEP94, Ref. GLS0579.

[34] DELPHI Collaboration, "A measurement of B meson production and lifetime using $D\ell^-$ events in Z decays," CERN-PPE/94-174.

[35] OPAL Collaboration, "Updated measurement of the B^0 and B^+ lifetimes including 1993 data," OPAL Physics Note PN149.

[36] DELPHI Collaboration, "A topological measurement of the lifetimes of charged and neutral B-hadrons," Glasgow ICHEP94, Ref. GLS0165, DELPHI 94-97, PHYS 414.

[37] CDF Collaboration, "Measurement of the B^+ and B^0 meson lifetimes," Glasgow ICHEP94, Ref. GLS0111.

[38] F. DeJongh, "Review of B^+ and B^0 lifetime measurements," presented at Glasgow.

[39] See, for example, Paula J. Franzini, Phys. Rep. **173**, 1 (1989).

[40] R. Forty, "CP violation and $B - \bar{B}$ mixing," CERN-PPE/94-154, presented at Glasgow, and references therein.

[41] OPAL Collaboration, "Measurement of the time dependence of $B^0_d\overline{B^0_d}$ mixing using a jet charge technique," CERN-PPE/94-43.

[42] ALEPH Collaboration, "The measurement of the time dependence of $B^0_d\overline{B^0_d}$ mixing using $D^\star$–lepton and $D^\star$–jet charge correlations," Glasgow ICHEP94, Ref. GLS 0576.

[43] OPAL Collaboration, "Measurement of the time dependence of $B^0_d\overline{B^0_d}$ mixing using leptons and $D^{\star\pm}$ Mesons," CERN-PPE/94-90.

[44] DELPHI Collaboration, "Measurement of time dependent $B^0_d\overline{B^0_d}$ mixing," Glasgow ICHEP94, Ref. GLS0171a, DELPHI 94-100, PHYS 417.

[45] DELPHI Collaboration, "New measurements of time dependent $B^0_d\overline{B^0_d}$ mixing with $D^\star$–hemisphere charge correlations," Glasgow ICHEP94, Ref. GLS0171b, DELPHI 94-101, PHYS 418.

[46] ALEPH Collaboration, "Measurement of the B^0_d oscillation frequency and a lower limit for the B^0_s," Glasgow ICHEP94, Ref. GLS0584.

[47] OPAL Collaboration, "A study of B meson oscillations using dilepton events" OPAL Physics Note PN152.

[48] DELPHI Collaboration, "Measurement of the B^0_d oscillation frequency using kaons, leptons, and jet charge," Glasgow ICHEP94, Ref. GLS0171c, DELPHI 94-118, PHYS 435.

[49] ALEPH Collaboration, Y. Pan, "Results on time-dependent $B^0\overline{B^0}$ mixing from ALEPH," presented at Glasgow.

[50] Particle Data Group, Phys. Rev. D **50**, 1173 (1994).

[51] ALEPH Collaboration, "Measurement of the Λ_b polarization at LEP," Glasgow ICHEP94, Ref. GLS0958.

[52] E. J. Eichten, C. T. Hill, and C. Quigg, Phys. Rev. Lett. **71** 4116 (1993).
S. Godfrey and R. Kokoski, Phys. Rev. D **43**, 43 (1991).

[53] ALEPH Collaboration, "Production of P-wave charmed mesons in Z decay," Glasgow ICHEP94, Ref. GLS0577.

[54] ALEPH Collaboration, "A study of $B^- \to (D^{\star+}\pi^-)\ell^-\bar{\nu}$ at LEP," Glasgow ICHEP94, Ref. GLS0608.

[55] OPAL Collaboration, "A study of charm meson production in semileptonic B decays," OPAL Physics Note PN144.

[56] ALEPH Collaboration, "$B^\star$ production in Z decays," Glasgow ICHEP94, Ref. GLS0598.

[57] L3 Collaboration, "B* production in Z decays at LEP," Glasgow.

[58] DELPHI Collaboration, "Excited beauty at DELPHI," Glasgow ICHEP94, Ref. GLS0305, DELPHI 94-80, PHYS 397.